

1
2
3
4
5
6
7
8
9
10
11
12
13
14
15
16
17
18
19
20
21
22
23
24
25
26
27
28
29

Sea ice break-up and freeze-up indicators for users of the Arctic coastal environment

John E. Walsh¹, Hajo Eicken¹, Kyle Redilla¹, Mark Johnson²

¹International Arctic Research Center, University of Alaska Fairbanks, Fairbanks AK 99775
USA

²College of Fisheries and Ocean Sciences, University of Alaska Fairbanks, Fairbanks AK
99775 USA

Correspondence to: John E. Walsh (jewalsh@alaska.edu)

September 2022

The Cryosphere, Revision 2

Formatted: Left: 1.19"

Deleted: July

Deleted: Revision for The Cryosphere

Formatted: Font: Italic

Formatted: Left

Formatted: Font: Italic

32

Abstract

33 The timing of sea ice retreat and advance in Arctic coastal waters varies substantially from year
34 to year. Various activities, ranging from marine transport to the use of sea ice as a platform for
35 industrial activity or winter travel, are affected by variations in the timing of break-up and
36 freeze-up, resulting in a need for indicators to document the regional and temporal variations in
37 coastal areas. The primary objective of this study is to use locally-based metrics to construct
38 indicators of break-up and freeze-up in the Arctic/Subarctic coastal environment. The indicators
39 developed here are based on daily sea ice concentrations derived from satellite passive
40 microwave measurements. The “day of year” indicators are designed to optimize value for
41 users while building on past studies characterizing break-up and freeze-up dates in the open
42 pack ice. Relative to indicators for broader adjacent seas, the coastal indicators generally show
43 later break-up at sites known to have landfast ice. The coastal indicators also show earlier
44 freeze-up at some sites in comparison with freeze-up for broader offshore regions, likely tied to
45 earlier freezing of shallow water regions and areas affected by freshwater input from nearby
46 streams and rivers. A factor analysis performed to synthesize the local indicator variations
47 shows that the local break-up and freeze-up indicators have greater spatial variability than
48 corresponding metrics based on regional ice coverage. However, the trends towards earlier
49 break-up and later freeze-up are unmistakable over the post-1979 period in the synthesized
50 metrics of coastal break-up/freeze-up and the corresponding regional ice coverage. The findings
51 imply that locally defined indicators can serve as key links between pan-Arctic or global
52 indicators such as sea-ice extent or volume and local uses of sea ice, with the potential to inform
53 community-scale adaptation and response.

54 *Key words:* sea ice, Arctic, break-up, freeze-up, ice concentration

Formatted: Justified

Deleted:

Deleted:

Deleted: is

Deleted:

Deleted: .

Deleted: extensive

Deleted: l

Deleted:

Deleted: the

64 **1. Introduction**

65 Coastal sea ice impacts residents and other users of the nearshore marine environment in
66 various ways. Perhaps most obvious is the fact that non-ice strengthened vessels require ice-
67 free waters for marine transport, which can serve purposes such as resupply of coastal
68 communities, the transport of extracted resources (oil, liquefied natural gas, mined metals),
69 migration of marine mammals (e.g., bowhead whales) and wintertime travel over the ice by
70 coastal residents. Key metrics for such uses of the nearshore marine environment are the
71 timing of break-up (or ice retreat) in the spring and the timing of freeze-up (or ice advance) in
72 the autumn or early winter.

73 Sea ice concentration thresholds have been used in various studies to determine the dates of
74 sea ice opening, retreat, advance and closing (Markus et al., 2009; Johnson and Eicken, 2016;
75 Bliss and Anderson, 2018; Peng et al., 2018; Bliss et al., 2019; Smith and Jahn, 2019). An
76 emerging tendency in these and similar studies is the definition of break-up date as the date on
77 which ice concentration drops below a prescribed threshold and remains below that threshold
78 for a prescribed minimum duration (chosen to eliminate repeated crossings of the
79 concentration threshold as a result of temperature- or wind-driven changes in ice coverage [in](#)
80 [response to](#) transient weather events). A corresponding criterion is used for the freeze-up date.

81 Coastal regions present special challenges in the application of such criteria. First, [landfast or](#)
82 [shorefast ice](#) (stationary sea ice held in place along the shoreline as a result of grounding
83 and/or confinement by the coast) is common in waters immediately offshore of the coast,
84 particularly in areas with shallow water. Landfast ice provides especially important sea ice
85 services because it offers a stable platform for nearshore travel, serves as a critical habitat for
86 marine mammals such as seals and polar bears (Dammann et al., 2018), and provides a buffer

Deleted: .(

Deleted: ,

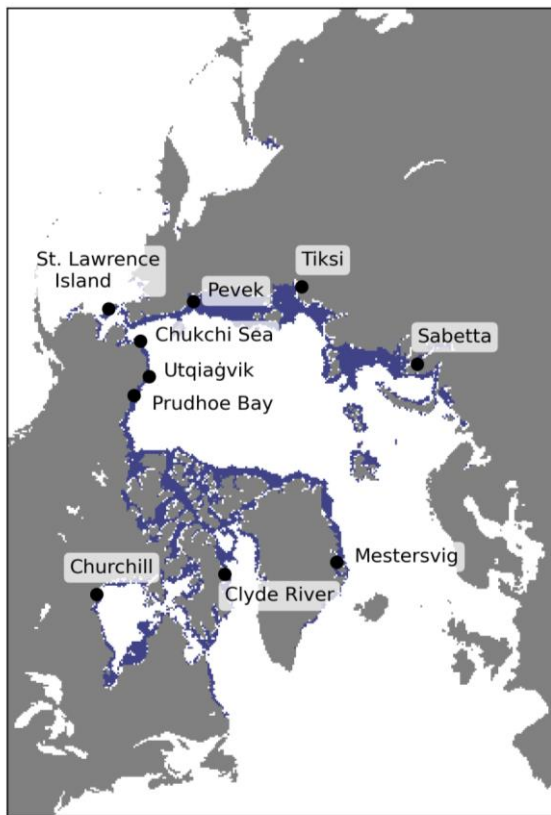
Deleted:). For example, Bliss et al. (2019) define dates of opening and retreat as, respectively, the last days on which the sea ice concentration drops below 80% and 15% before the summer minimum. Corresponding metrics are used by Bliss et al. for the dates of advance and closing.

Deleted: associated with

Deleted: or landfast

Deleted: (Fig. 1-formerly 15).

97 against coastal storms (Hosekova et al., 2021). Landfast ice extends offshore by hundreds of
98 meters to many tens of kilometers. Figure 1 shows the geographical distribution of landfast ice
99 in terms of the maximum extent during June for the period 1972-2007. Landfast ice is most
100 extensive over shallow waters of the Siberian Seas and the Canadian Archipelago. Given its
101 widespread presence at coastal sites in the Arctic, landfast ice will be a key feature in our
102 assessment of any differences in the sea-ice indicators, particularly for ice break-up, when
103 comparing coastal to offshore regions.



104

105 Figure 1. Landfast ice distribution shown as the maximum extent of landfast ice over the
106 1972-2007 period. Data source: National Ice Center via National Snow and Ice Data Center,
107 NSIDC dataset G02172 -- <https://nsidc.org/data/G02172> (accessed 4 September 2022).

Formatted: Font:

108 A second challenge associated with coastal regions is that sea ice concentrations derived from
109 passive microwave measurements are prone to contamination by microwave emissions from
110 land in coastal grid cells. Additionally, many parts of the Arctic coastline have inlets, river
111 deltas and barrier islands that are not captured by the 25 km resolution of the passive
112 microwave product. While higher-resolution datasets permitting finer resolution of coastal sea
113 ice are available from sensors such as AMSR (Advanced Microwave Scanning Radiometer),
114 the record lengths are sufficiently shorter (about 20 years for AMSR) that trend analyses are
115 limited by a reliance on such products. Trend analysis is one of the main components of the
116 present study.

Deleted: Second,

Deleted: Finally

117 A pervasive finding from recent studies of trends in Arctic sea ice is a shortening of the sea
118 ice season. This finding is often presented in terms of the corresponding lengthening of the
119 open water season (e.g., Stroeve et al., 2014; Stroeve and Notz, 2018; Onarheim et al., 2018;
120 Bliss and Anderson, 2018; Peng et al., 2019; Smith and Jahn, 2019). Because the reduction of
121 ice extent has been greater in summer than in winter, the percentage of the Arctic sea ice
122 cover experiencing break-up and freeze-up (i.e., the percentage of the maximum ice cover that
123 is seasonal) has increased from about 50% in 1980 to more than 70% in recent years
124 (Druckenmiller et al., 2021; Thomson et al., 2022). Since 1980, the length of the open water
125 period has increased by between one and two months (over 10 days per decade)
126 (Stammerjohn et al., 2012; Peng et al., 2019; Thomson et al., 2022), with contributions of
127 comparable magnitude from earlier break-up and later freeze-up. Regional variations of these

Moved (insertion) [2]

Deleted: The lengthening of the open-water season

Deleted: in the Arctic has been well-documented

Deleted: As a result

133 trends, both in the vicinity of the coasts and in regions farther offshore, are the focus of this
134 paper as well as Bliss et al. (2019), to which we will compare our results.
135 Trends in freeze-up have been shown previously to be sensitive to the criterion for freeze-up
136 (Peng et al., 2018; Bliss et al., 2019). For example, Peng et al. (2018) found that the trends in
137 the autumn crossing of the 80% concentration were greater than trends in the crossing of the
138 15% threshold (Thomson et al., 2022), implying a slowing of the autumn/winter ice advance.
139 Such findings, as well as those of Johnson and Eicken (2016), motivate our use of separate
140 indicators for the start and end of break-up and freeze-up.
141 The delayed autumn freeze-up is a manifestation of the release of increased amounts of heat
142 stored in the upper layers of the ocean, largely as a result of the increased solar absorption
143 made possible by the earlier break-up. In this respect, trends in break-up and freeze-up are
144 intertwined. This linkage has been demonstrated quantitatively by Serreze et al. (2016) and
145 Stroeve et al. (2016), who explored the use of break-up timing as a predictor of the timing of
146 ice advance in the Chukchi Sea and the broader Arctic, respectively.
147 The primary objective of this study is to use the locally-based metrics to construct indicators
148 of break-up and freeze-up on Arctic/Subarctic coastal environments. A secondary objective is
149 to contribute to efforts at the national and global scale to establish key sets of indicators that
150 support sustained assessment of climate change and inform planning and decision-making for
151 adaptation action (AMAP, 2018; IPCC, 2022). At the global, pan-Arctic, and U.S. national
152 levels, indicators associated with the state of the sea ice cover so far have focused on the
153 summer minimum and winter maximum extent and ice thickness (IPCC, 2022; AMAP, 2017;
154 Box et al., 2019; USGCRP, 2017). As outlined by Box et al. (2019), this approach has been
155 motivated by the objective of describing and tracking the state of key components of the

Deleted: have

Deleted: d

Deleted: have

Deleted: d

Deleted: ¶

Deleted: was

Deleted: subcomponent of this overall

163 global climate system. However, large-scale (pan-Arctic) measures of e.g., sea-ice extent or
164 volume are of little value and relevance to those needing to adapt or respond to such change at
165 the community or regional scale. Here, we examine the timing of sea-ice freeze-up and break-
166 up as key constraints for a range of human activities and ecosystem functions in Arctic
167 settings.

168 2. Data and methods

169 The primary data source is the archive of gridded daily sea ice concentrations derived from
170 the SMMR, SSM/I and SSMIS sensors onboard the Nimbus-7 and various DMSP satellites
171 dating back to November, 1978. The dataset is NSIDC-0051 of the National Snow and Ice
172 Data Center (NSIDC) and is accessible at <https://nsidc.org/data/nsidc-0051>. In the
173 construction of this dataset, the NASA Team algorithm (Cavalieri et al., 1984) was used to
174 process the microwave brightness temperatures into a consistent time series of daily sea ice
175 concentrations. The data are on a polar stereographic grid projection with a grid cell size of 25
176 km x 25 km. Prior to [computing the break-up and freeze-up metrics described below](#), the data
177 were processed with a linear interpolation to fill in missing daily values, followed by a spatial
178 and then temporal smoothing to filter out short (< 3 days) events. Specifically, the daily sea
179 ice concentration values were spatially smoothed using a [generic boxcar](#) filter with a square
180 footprint of 3 x 3 grid cells. The data were then temporally smoothed three times using a Hann
181 window.

182 The daily sea ice concentrations are used to define the metrics of the start and end of break-up
183 and freeze-up in each year of a 40-year period, 1979-2018. The definitions build on those
184 used by Johnson and Eicken (2016; hereafter denoted as J&E), which were informed by
185 Indigenous experts' observations of ice use and ice hazards in coastal Alaska, and relate to

Deleted: and the NASA Bootstrap algorithm (Comiso et al., 1986) were

Deleted: applying these definitions

Deleted: generic mean

190 planning and decision-making at the community-scale (Eicken et al., 2014). Here, we expand
191 the satellite data analysis with minor modifications of the break-up and freeze-up criteria to
192 broaden the applicability to coastal areas. Examples include imposing maximum and
193 minimum values for the thresholds computed from summary statistics of the daily sea ice
194 concentration values of relevant periods. The revised definitions are presented in Table 1 and
195 the differences relative to those of J&E are listed in Table 2.

196 The four indicators in this study are the dates of the start and end of break-up and freeze-up.
197 For purposes of this study, the break-up period may be regarded as the time between the
198 Arctic sea ice maximum (typically in March) and the sea ice minimum (typically in
199 September, with June representative of the period most rapid break-up). Similarly, the freeze-
200 up period extends from September through March, with November representative of the
201 period of most rapid freeze-up. The corresponding indicators used by Bliss et al. (2019) are
202 the date of opening (defined as the last day on which the ice concentration drops below 80%
203 before the summer minimum), the date of retreat (defined as the last day the ice concentration
204 drops below 15% before the summer minimum), the date of advance (defined as the first day
205 the ice concentration increases above 15% following the final summer minimum) and the date
206 of closing (defined as the first day the ice concentration increases above 80% following the
207 final summer minimum). For the comparisons of indicator dates presented in Section 3, we
208 did not make any modifications to the Bliss et al. (2019) criteria.

209 While the various thresholds in Table 1 may seem somewhat arbitrary at first glance, they are
210 based on past sensitivity tests. In particular, the 10% threshold is based on prior work (J&E)
211 in which sensitivities were explored. The selected thresholds were those that generally
212 maximized the number of such years across the coastal locations and MASIE regions.

Moved (insertion) [1]

Deleted: ¶

Deleted: studies and subsequent

Deleted: The 25%, 40% and 50% thresholds in Table 1 were arrived at by testing various values and selecting values that maximized the number of years with break-up and defined freeze-up dates and had the best agreement with years of indigenous observations. The

Formatted: Font: (Default) Times New Roman, 12 pt

Formatted: Font: (Default) Times New Roman, 12 pt

Deleted: values

Deleted: various

Deleted: ¶

¶

¶

¶

¶

¶

229 Table 1. Definition of the start and end of break-up and freeze-up.

230	Break-up start	The date of the last day for which the previous two weeks' ice concentration
231		always exceeds a threshold computed as the maximum of (a) the winter
232		(January-February) average minus two standard deviations and (b) 15%.
233		Undefined if the average summer sea ice concentration (SIC) is greater than
234		40% or if the subsequent break-up end is not defined.
235	Break-up end	The first date after the break-up start date for which the ice concentration
236		during the following two weeks is less than a threshold computed as the
237		maximum of (a) the summer (August-September) average plus one standard
238		deviation and (b) 50%. Undefined if the daily SIC is less than the threshold
239		for the entire summer or if break-up start is not defined.
240	Freeze-up start:	The date on which the ice concentration exceeds for the first time a threshold
241		computed as the maximum of (a) the summer (August-September) average
242		plus one standard deviation and (b) 15%. Undefined if the daily SIC never
243		exceeds this threshold, if the mean summer SIC is greater than 25%, or if
244		subsequent freeze-up end is not defined.
245	Freeze-up end:	The first date after the freeze-up start date for which the following two
246		weeks' ice concentration exceeds a threshold computed as the maximum of
247		(a) the average winter (January-February) ice concentration minus 10% and
248		(b) 15%, and the minimum of this result and (c) 50%. Undefined if daily SIC
249		exceeds this threshold for every day of the search period or if freeze-up start
250		is not defined.

251 Table 2. Changes in the indicator definitions relative to Johnson and Eicken (2016), denoted
252 as “J&E”. The symbol “ σ ” denotes standard deviation; “sic” denotes sea ice concentration.

253 *Break-up start:*

- 254 - minimum sic threshold created at 15% (J&E: last day exceeding Jan-Feb mean minus 2σ)
- 255 - undefined if average summer sic > 40% (J&E: no such criterion)
- 256 - undefined if subsequent breakup end date not defined (J&E: no such criterion)

257

258 *Break-up end:*

- 259 - first time sic below threshold for 2 weeks instead of last day below threshold
260 (J&E: last exceeding larger of Aug-Sep mean or 15%)
- 261 - minimum threshold 50% (J&E: minimum threshold of 15%)
- 262 - undefined if break-up start not defined (J&E: no such criterion)

263

264 *Freeze-up start:*

- 265 - first day on which sic exceeds Aug-Sep average by 1σ (J&E: same)
- 266 - undefined if mean summer sic > 25% (J&R: no such criterion)
- 267 - undefined if subsequent freeze-up end not defined (J&E: same)

268

269 *Freeze-up end:*

- 270 - first time sic above threshold for following 2 weeks instead of first day above threshold
271 (threshold is Jan-Feb average minus 10%, as in J&E)
- 272 - thresholds imposed: Minimum (15%) and maximum (50%) (J&E: no such thresholds)
- 273 - undefined if sic always exceeds threshold (J&E: same)

274 Our evaluation of the coastal indicators includes comparisons of the various dates (break-
275 up/freeze-up start/end) at nearshore locations with the corresponding metrics for broader areas
276 of the Arctic Ocean and the subarctic seas. A set of ten locations was selected on the basis of
277 their geographical distribution and the relevance of local sea ice to uses by communities,
278 industry, military or other stakeholders. Examples of local uses include over-ice travel for
279 access to marine mammals, offshore travel between coastal communities, access of coastal
280 facilities by commercial vessels, and protection from coastal waves and erosion. The ten
281 locations are shown in Figure 2 and listed in Table 3, together with their geographic
282 coordinates. While there is admittedly some subjectivity in the selection of these sites, our
283 priorities were (1) a pan-Arctic geographical distribution, thereby expanding the emphasis on
284 North American locations in past studies (see Discussion in Section 4) and (2) inclusion of
285 locations with a mix of users affected by sea ice: Indigenous communities, industry, military
286 and other stakeholders. For each of these locations, several passive microwave grid cells close
287 to (but not adjacent to) the coastline were selected for calculation of the break-up and freeze-
288 up metrics. More specifically, the contamination of the passive microwave-derived ice
289 concentrations by the presence of land in a grid cell required the exclusion of grid cells
290 containing land. Therefore, the selected grid cells satisfied the criterion that they were the
291 cells closest to the coast but centered at least 25 km from the coast. Figure 2 shows
292 geographical insets illustrating the proximity of the selected grid cells to the coastline.

293 With regard to the grid cell selection, we experimented with the grid cell selections at Sabetta
294 and Utqiagvik. When the grid cell locations were shifted offshore by one pixel at Sabetta, the
295 mean break-up start and end dates changed by only -0.1 and -1.1 days, respectively; the
296 corresponding changes in the freeze-up start and end dates were 0.2 and -0.7 days,

Deleted: These

Deleted: 1

Deleted: 1

300 respectively. At Utqiagvik, the offshore shift resulted in an earlier mean break-up start by 3.3
 301 days and a later mean break-up end by 2.9 days. The earlier break-up start is consistent with
 302 the presence of fast ice at the coast, as discussed in Section 4. The changes in Utqiagvik's
 303 freeze-up dates were small when the pixels were shifted offshore, where the start of freeze-up
 304 occurred 1.1 days later and the end of freeze-up 1.1 days earlier than closer to the coast.

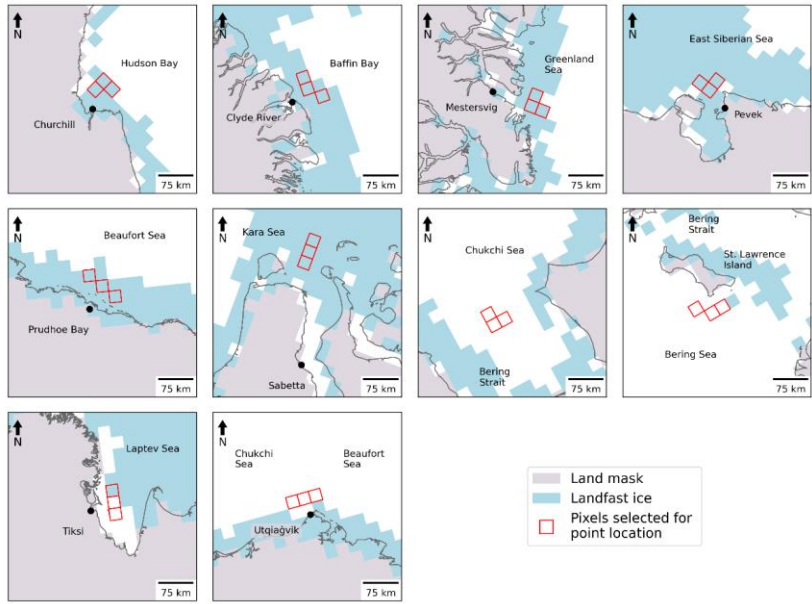
Deleted: ¶

Formatted: Space Before: Auto, After: Auto

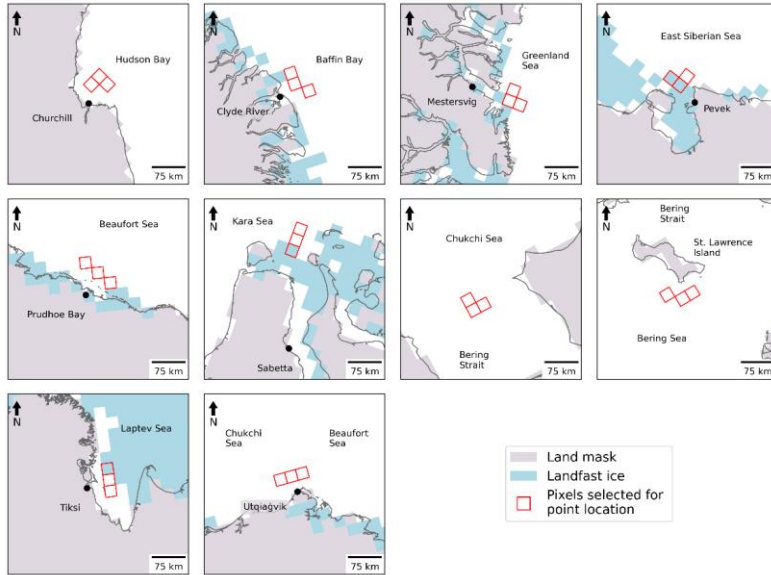
306 Table 3. Near-coastal locations selected for calculation of break-up and freeze-up metrics

307	<u>Sea</u>	<u>Location</u>	<u>Latitude, Longitude</u>	<u>Significance of location</u>
308	Beaufort Sea	Prudhoe Bay	70.2N, 148.2W	oil facilities
309	Chukchi/Beaufort Seas	Utqiagvik	71.3N, 156.8W	Indigenous community
310	Chukchi Sea	Chukchi Sea	69.6N, 170W	shipping route
311	Bering Sea	St. Lawrence Island	65.7N, 168.4W	Indigenous community
312	East Siberian Sea	Pevek	69.8N, 170.6E	port, mining facility
313	Laptev Sea	Tiksi	71.7N, 72.1E	research site, port
314	Kara Sea	Sabetta	71.3N, 72.1E	port, LNG facility
315	Greenland Sea	Mestersvig	72.2N, 23.9W	military base
316	Baffin Bay	Clyde River	70.3N, 68.3W	Indigenous community
317	Hudson Bay	Churchill	58.8N, 94.2W	port, tourism

319



320



321

322 Figure 2. Grid cells (red squares) for which passive-microwave-derived ice concentrations
 323 were used in computing the break-up and freeze-up metrics for the coastal locations. Black
 324 dots represent the actual locations of the coastal communities. Blue shading denotes
 325 maximum (upper panels) and median (lower panels) coverage of landfast ice in June over the
 326 1972-2007 period based on charts of the U.S. National Ice Center --
 327 <https://nsidc.org/data/G02172> (accessed 28 June 2022).

328 It is apparent from Figure 2 that the innermost extent of the landfast ice does not always
 329 coincide with the coastline, which we assume here should always be the inner boundary of
 330 landfast ice. The northern Siberian coast (Sabetta and Tiksi) provides examples. In pursuing
 331 an explanation for the discrepancies, we found that the land mask in the fast ice dataset
 332 (digitized charts of the National Ice Center) differs from the land mask of the NSIDC's

Deleted: 1

Moved (insertion) [3]

Moved (insertion) [4]

Deleted: Figure 15 shows the median and maximum extent of landfast ice during June for the period 1972-2007. Landfast ice is most extensive over shallow waters of the Siberian Seas and the Canadian Archipelago, although it can develop in the general vicinity of all of our sites (Fig. 1), with the exception of the offshore location in the Chukchi Sea. Given its widespread presence at the coastal sites in the Arctic, landfast ice a key feature in our assessment of coastal-offshore differences in particular for ice break-up. It is for this reason that we have attempted to place our findings into a context of landfast ice.

Maximum climatology

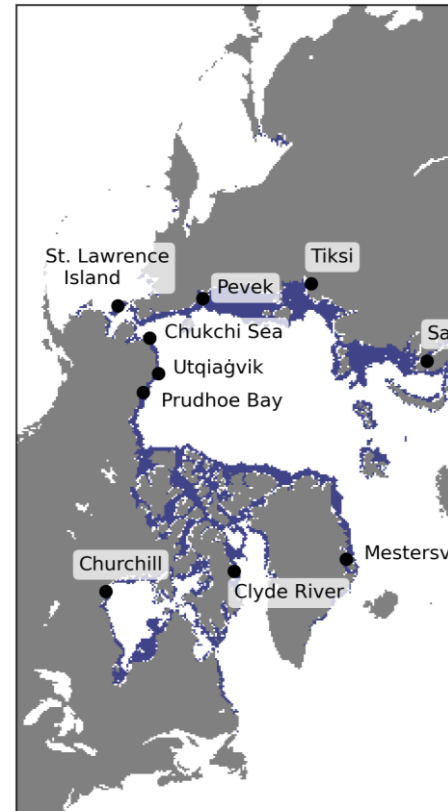


Figure 15. Landfast ice climatology for June based on the digitized ice charts of the National Ice Center. Blue shading denotes median extent (left panel) and maximum extent (right panel) of landfast ice over the 1972-2007 period. Data source: National Ice Center via ...

Formatted: Font:

Deleted: 1

367 passive microwave dataset. The resulting offset does not change the area covered by sea ice in
368 each regional plot, but it does result in the mis-location of the [inner boundary of landfast ice](#),

369 The discrepancy does not alter the reasoning about the geographically varying roles of

370 landfast ice, as discussed in Section 4, [and a more detailed analysis of the origin of these](#)

371 [offsets in coastline depiction and landfast ice location](#) is beyond the scope of this paper.

Deleted: nearshore edge

Deleted: .

Deleted: relative to the coastline

372 The grid cell selections for St. Lawrence Island and the Chukchi Sea deserve special
373 comment. The grid cells off St. Lawrence Island were chosen to reflect timing and location of
374 subsistence harvests by the communities of Gambell and Savoonga. Because of extensive ice
375 coverage, including landfast ice, north and northwest of the island, both communities
376 traditionally conduct bowhead whale harvests at hunting camps on the south side of the island
377 once spring ice break-up is underway (Noongwook et al., 2007). These sites also reflect the
378 seasonal migration of whales in waters south of the island with the seasonal retreat of the ice
379 cover (Noongwook et al., 2007), modulated somewhat by the presence of a polynya south and
380 southwest of the island (Krupnik et al., 2010; Noongwook et al., 2007). Traditional walrus
381 harvest practices on St. Lawrence Island await the very end of the bowhead whale hunt
382 (Kapsch et al., 2010), with timing of spring ice break-up south of the island as the driving
383 factor. These practices motivated our selection of grid cells southeast of the island. As shown
384 later (Section 4), landfast ice is confined to the northern coastal region of St. Lawrence Island
385 – consistent with the frequent presence of the polynya south of the island. In the case of the
386 Chukchi Sea, the grid cells are indeed farther from the coast than for the other sites; the
387 locations were intentionally selected to be farther offshore in order to provide a non-coastal
388 counter-example to the other sites, all of which are adjacent to a coast.

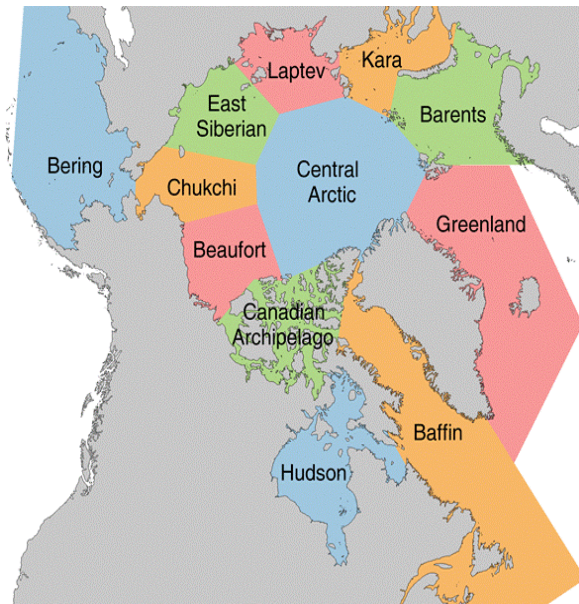
392 Previous studies cited earlier have evaluated break-up and freeze-up metrics for subregions of
393 the Arctic Ocean and the surrounding seas (Markus et al., 2006; Johnson and Eicken, 2016;
394 Bliss and Anderson, 2018; Peng et al., 2018; Bliss et al., 2019; Smith and Jahn, 2019). For
395 comparisons with broader regions offshore of our selected sites, we utilize the MASIE
396 (Multisensor Analyzed Sea Ice Extent) regionalization
397 (https://nsidc.org/data/masie/browse_regions). Of the MASIE regions shown in Figure 3, we
398 choose the following for computation of regionally averaged metrics of break-up and freeze-
399 up: Beaufort Sea, Chukchi Sea, East Siberian Sea, Laptev Sea, Kara Sea, Greenland Sea,
400 Baffin Bay, Hudson Bay, and Bering Sea.

Formatted: Indent: First line: 0"

Deleted: 2

Deleted: (8)

Deleted: ¶



401

402 Figure 3. The MASIE subregions of the Arctic. Regions utilized in this study include
403 Beaufort Sea, Chukchi Sea, East Siberian Sea, Laptev Sea, Kara Sea, Baffin Bay, Hudson
404 Bay, and Bering Sea.

Deleted: 2

409 The following section includes time series of the local indicators and, for comparison, time
410 series of the corresponding MASIE regional indicators. In order to address the spatial
411 coherence of the indicators, we performed a factor analysis on the different sets (break-
412 up/freeze-up, start/end dates). The computation of the indicators was done for the [jen](#) local
413 sites and for the MASIE regions in which they fall. Factor analysis is a statistical method for
414 quantifying relationships among a set of variables. The variability in the overall dataset is
415 depicted by a set of factors. Each factor explains a percentage of the total variance in space
416 and time. Each variable in each factor is given a loading (or weight) based on its contribution
417 to the variance explained by that factor. The first factor can be viewed as the linear
418 combination of the variables that maximizes the explained variance in the overall dataset. The
419 second and each successive factor maximize the variance unexplained by the preceding
420 factors. Successive factors explain successively smaller fractions of the overall variance.
421 Multiple variables can have strong loadings in the same factor, indicating they follow a
422 similar pattern and are likely highly related. Factor analysis has a long history of applications
423 to Arctic sea ice variability (Walsh and Johnson, 1982; Fang and Wallace, 1994; Deser et al.,
424 2000; Fu et al., 2021). The factor analysis calculations used here were performed using the
425 XLSAT software package run in Excel (<https://www.xlstat.com/en/>)

Deleted: tem

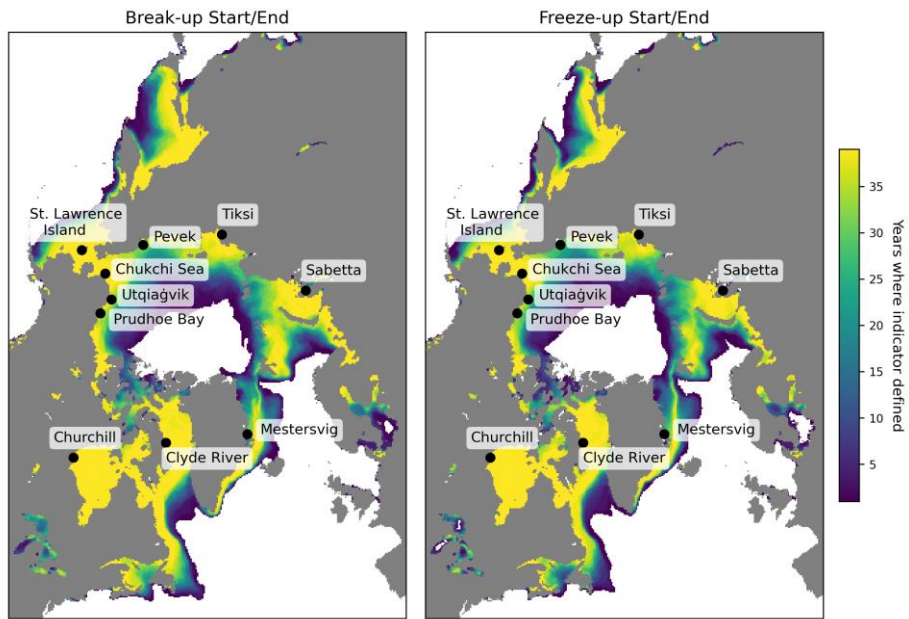
426 **3. Results**

427 With coastal ice retreat and onset of ice advance as this study's primary foci, we first
428 demonstrate the applicability of the indicators evaluated here. The various metrics of sea ice
429 break-up and freeze-up in Table 1 are not defined for all locations in the Arctic. For example,
430 locations that remain ice-covered throughout a particular year will not be assigned dates for
431 any of the indicators in that year, and the same is true of locations at which sea ice does not

433 form during a particular year. Figure 4 shows the number of years in the 1979-2018 study
 434 period during which the break-up and freeze-up indicators are actually defined. It is apparent
 435 that the indicators are consistently defined in the seasonal sea ice zone spanning the subarctic
 436 seas. In particular, all ten coastal locations in Table 2 are in the yellow areas (>35 years out of
 437 40 years defined) of Figure 4. Of note in Figure 4 is that the number of years with defined
 438 break-up indicators slightly exceeds (by one) the number of years with freeze-up indicators at
 439 some locations at the outer periphery of the seasonal sea ice zone. These are locations in
 440 which sea ice was present for some portion of the early years but not at the end of the study
 441 period, so in one of the years there was a break-up but no freeze-up.

Deleted: 3

Deleted: 3
 Deleted: 3



442

443 Figure 4. Number of years in the 1979-2018 study period in which the break-up and freeze-up
 444 indicators were defined. Note that end dates for break-up and freeze-up exist only for years in

Deleted: 3

449 which there are start dates for break-up and freeze-up. The start and end dates of the overall
450 data record (1 Jan 1979 – 31 Dec 2018) can result in differences of 1 year in the counts when
451 freeze-up occurs around January 1.

452

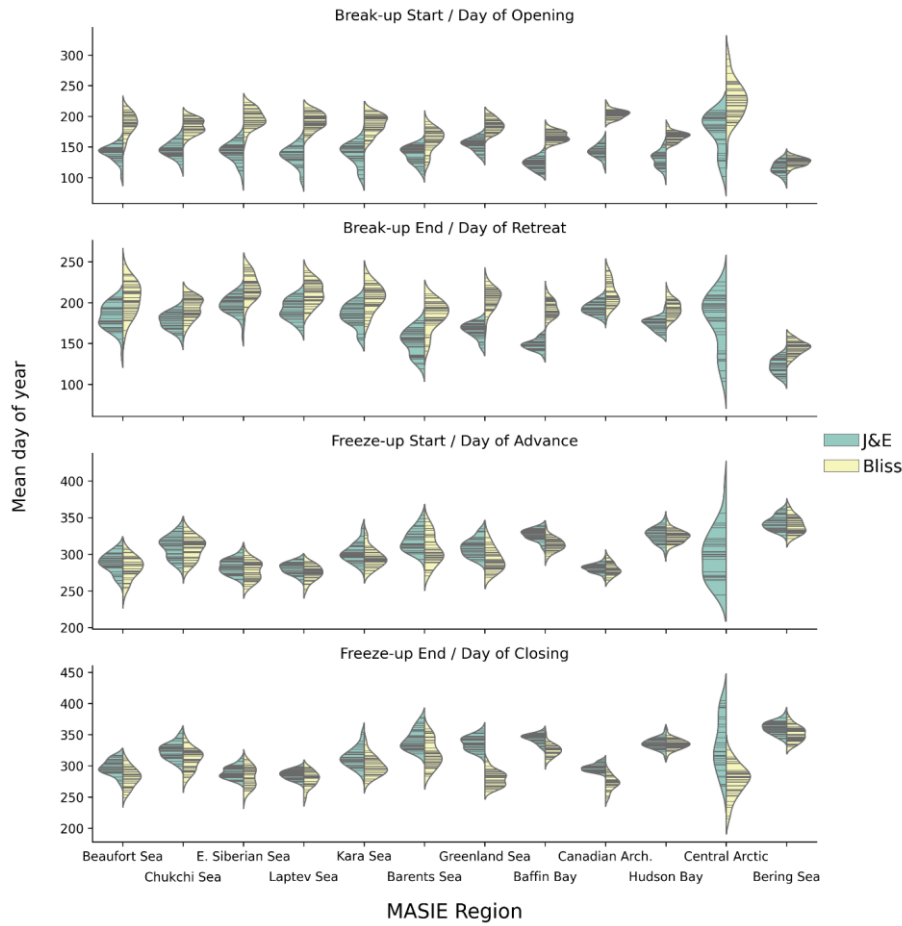
453 A key issue to be addressed is the degree to which the indicators utilized here differ from
454 those of previous studies. The metrics of Bliss et al. (2019) or similar variants have been used
455 in recent publications and provide natural points of comparison. While there are various
456 differences between our metrics and those of Bliss et al., the most consequential for the
457 computed dates is the use of departures from winter/summer averages concentrations in our
458 criteria vs. Bliss et al.'s use of 15% and 80% concentrations as key thresholds. This
459 distinction is analogous to the difference between the NASA Team algorithm's use of fixed
460 tie points and the NASA Bootstrap algorithm's use of "dynamic" (time/space-varying) tie
461 points.

462 Figure 5 and Table S1 show that there are systematic differences between our metrics (based
463 on the modified J&E criteria) and those of Bliss et al. when the two sets of metrics are
464 evaluated for the MASIE regions. In particular, J&E's start and end of breakup generally
465 occur earlier by up to several weeks than the corresponding dates of opening and retreat
466 defined by Bliss et al. On the other hand, J&E's freeze-up dates are more closely aligned with
467 those of Bliss et al., although J&E's end-of-freeze-up occurs later (by 1 to 3 weeks) than Bliss
468 et al.'s closing date in most of the MASIE regions, especially the North Atlantic and Canadian
469 regions.

Moved up [1]: The four indicators in this study are the dates of the start and end of break-up and freeze-up. The corresponding indicators used by Bliss et al. (2019) are the date of opening (defined as the last day on which the ice concentration drops below 80% before the summer minimum), the date of retreat (defined as the last day the ice concentration drops below 15% before the summer minimum), the date of advance (defined as the first day the ice concentration increases above 15% following the final summer minimum) and the date of closing (defined as the first day the ice concentration increases above 80% following the final summer minimum).

Deleted: 4

Deleted: J&E



484

485 Figure 5. “Violin” plots of the Julian dates of the break-up/freeze-up metrics used in this
 486 study based on Johnson and Eicken (2016) (green shading) and the corresponding dates of ice
 487 opening, retreat, advance and closing as defined by Bliss et al. (2019) (yellow shading). A
 488 violin plot shows a distribution by widening the horizontal lines in the ranges (of day of the
 489 year, in this case) having the highest concentration of values. The thin black lines represent

Formatted: Space After: 18 pt

490 the observations themselves; the black strips are clusters of lines representing groups of
491 similar values in the distribution. The violin plots provide no information about the temporal
492 sequence of the values.

493 The violin plots in Figure 5 show distributions but not the temporal variations that have been
494 indicated by results of previous studies (Peng et al., 2018; Bliss et al., 2019). Figures 6 and 7
495 provide the temporal perspective on the end dates of break-up (Day of retreat) and freeze-up
496 (Day of closing), respectively. In each of the MASIE regions, the J&E criterion gives an
497 earlier break-up date. The difference is typically two to three weeks, although it exceeds a
498 month in the Greenland Sea and Baffin Bay. Despite the offsets, the trends are nearly the
499 same in nearly all the regions. Exceptions are the Canadian Archipelago, where the J&E trend
500 is weaker than the Bliss trend, and the Bering Sea, where the trends are opposite in sign.
501 However, the trend in the Bering region is not statistically significant at the 99% level by
502 either metric, in contrast to all other regions in which the trends are significant at this level
503 (Table S2). The main conclusion from Figure 6 is that, except for the Bering Sea, sea ice
504 break-up is occurring earlier throughout the Arctic than several decades ago, no matter which
505 metric is used.

506 In contrast to the trends towards earlier breakup, the J&E and Bliss metrics for the end of
507 freeze-up both show significant trends towards later dates in most of the MASIE regions
508 (Figure 7 and Table S3). In this case, even the Bering Sea shows a trend towards later freeze-
509 up. Again, there is an offset towards a later date with the J&E metric, although the offset has
510 a range among the regions, from essentially zero in Hudson Bay to more than six weeks in the
511 Greenland Sea. The trends, however, show less agreement in some regions than do the trends
512 for break-up dates in Figure 6. The J&E trends are less positive than the Bliss trends in the

Deleted: 4

Deleted: 5

Deleted: 6

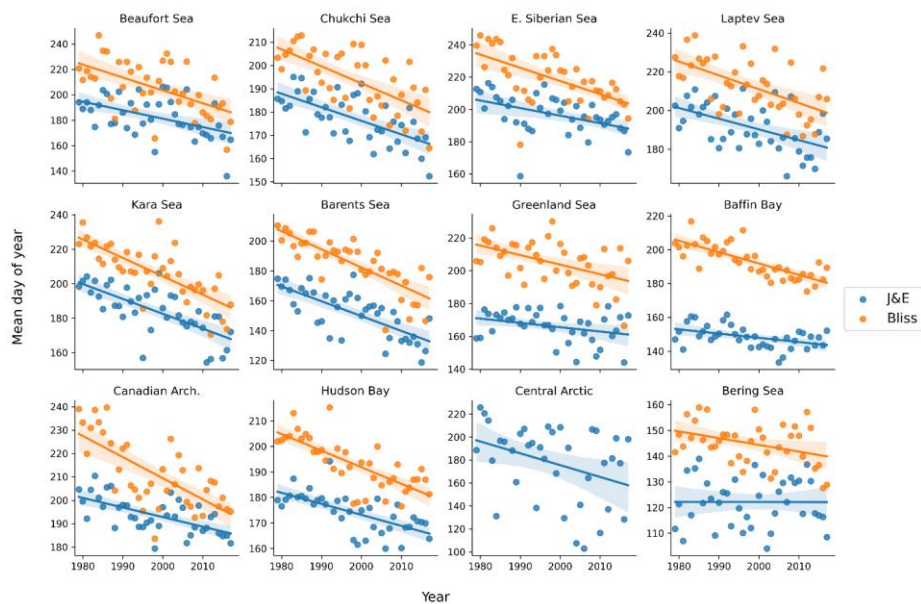
Deleted: 5

Deleted: 6

Deleted: 5

Deleted: more strongly

520 seas of the eastern Russian sector: the Chukchi, East Siberian and Laptev Seas. The same is
 521 true, although to a lesser degree, in the Barents Sea and the Canadian Archipelago. The main
 522 message from Figure 7 is that the freeze-up is ending later throughout the Arctic, although the
 523 magnitude of the trend is more sensitive to the criteria used for end-of-freeze-up than for end-
 524 of-break-up.



526
 527 Figure 6. Yearly values of J&E’s break-up end date (blue symbols) and the Bliss et al.’s
 528 (2019) Day of retreat (orange symbols) in the various MASIE regions. Corresponding trend
 529 lines are shown in each panel. (For the Central Arctic region, Bliss et al.’s “Day of retreat”
 530 metric is not shown because it was defined for fewer than half the years). Y-axis labels
 531 represent day of the year. Date scales on y-axis vary among panels in order to optimize
 532 display of data points. For numerical values of slopes and significance levels, see Table S2.

Deleted: 6
 Deleted: ¶

Break
 300
 250
 200
 150
 100

Brea
 250
 200
 150
 100

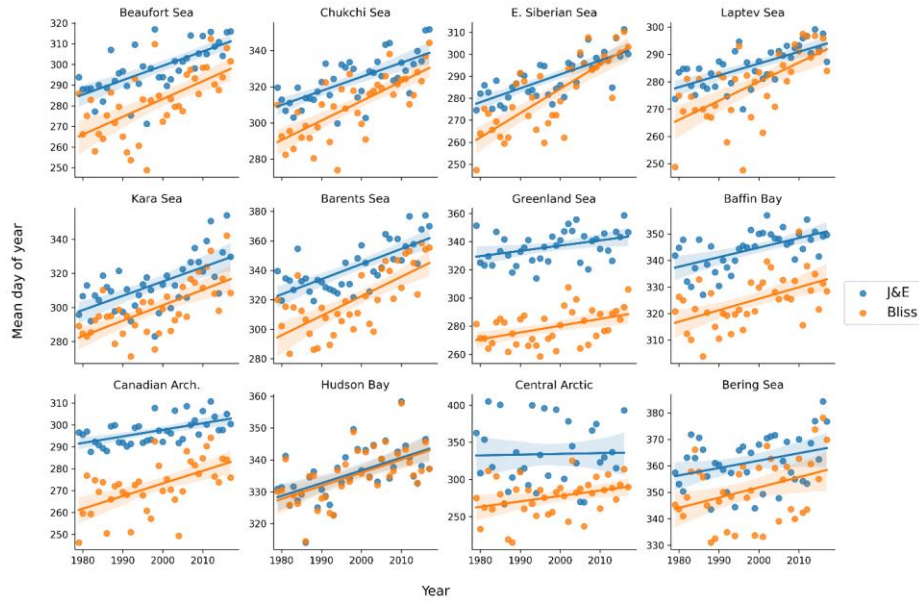
Freeze
 400
 350
 300
 250
 200

Freez
 450
 400
 350
 300
 250
 200

Beaufort Sea E. Siberian Sea Kara Si
 Chukchi Sea Laptev Sea

Deleted:
 Deleted: 5
 Deleted: the
 Deleted: metric
 Deleted: (
 Deleted:)
 Deleted: was not defined for a sufficient number of years
 Deleted: Numerical
 Deleted: their
 Deleted: are provided in

558



559

560 Figure 7. Yearly values of J&E’s freeze-up end date (blue symbols) and the Bliss et al.’s
561 (2019) Day of closing (orange symbols) in the various MASIE regions. Corresponding trend
562 lines are shown in each panel. Y-axes labels represent day of the year. Date scales on y-axis
563 vary among panels in order to optimize display of data points. Numerical values of slopes and
564 their significance levels are provided in Table S3.

565

566 A final comparison is presented in Figure 8, which shows the ice season lengths computed
567 using the two sets of metrics. The ice season length is defined as the number of days between
568 the end of freeze-up and the start of break-up. Consistent with J&E’s earlier break-up (Figure
569 6) and later freeze-up (Figure 7), the J&E metrics yield a shorter ice season than the Bliss et al
570 metrics. The differences in Figure 8 exceed a month in most of the Arctic except for the

Deleted: 6

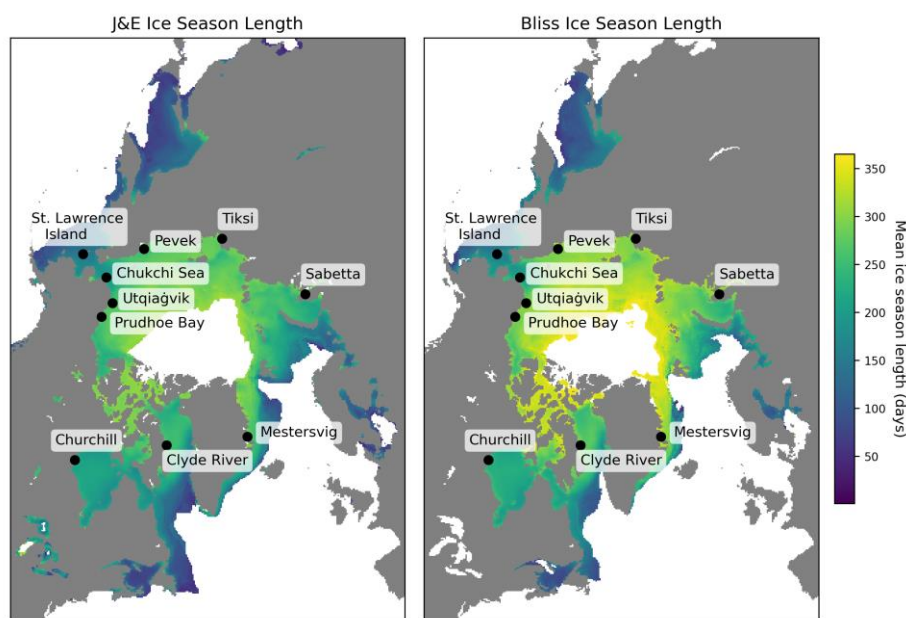
Deleted: 7

Deleted: 5

Deleted: 6

Deleted: 7

576 Bering Sea, Hudson Bay and the Canadian Archipelago. However, the negative trends of ice
577 season length are similar in magnitude according to both sets of metrics over most of the
578 Arctic. The trend maps are not shown here because they add little to the information conveyed
579 in Figures 6 and 7.



580
581 Figure 8. Mean ice season length based on the J&E metrics (left) and the Bliss et al. (2019)
582 metrics (right). Metrics of break-up and freeze-up were not defined in a sufficient number of
583 years in the white area near the North Pole.

584 Given that [this study targets the use of local indicators](#), it is important to assess the
585 relationship between the local indicators and those for the broader MASIE regions containing
586 the coastal locations. [An important caveat in such a comparison is that our local indicators](#)

Deleted: 5

Deleted: 6

Deleted: 7

Deleted: the development of local indicators is a main objective of this study

Deleted:

593 were designed for coastal users, not for broader regional or applications in areas far from
594 shore. This distinction introduces the possibility that the coastal indicators may be less than
595 optimal for the larger MASIE regions. Figures 9-10 provide these comparisons for the break-
596 up metrics defined by the modified J&E algorithms. In all cases, the yearly values (and linear
597 trend lines) for the ten coastal locations in Table 3 are plotted for the 1979-2018 period,
598 together with the values for the corresponding MASIE regions.

Deleted: 8-11

Deleted:

Deleted: all four

599 The break-up start dates (Figure 9) differ between the coastal locations and the broader
600 MASIE regions in most of the ten cases, and in some cases the trends are notably different.
601 With regard to systematic differences, not only the magnitude but also the sign of the offsets
602 varies among the regions. The break-up start date at the coast is later than for the MASIE
603 regions for Prudhoe (Beaufort Sea), Utqiaġvik (Chukchi Sea), Tiksi (Laptev Sea), and both
604 Canadian locations: Churchill (Hudson Bay) and Clyde River (Baffin Bay). These sites are all
605 Arctic coastal locations at which varying extents of landfast ice are present. By contrast, the
606 coastal locations have earlier break-up start dates (relative to their corresponding MASIE
607 regions) at St. Lawrence Island, Mestersvig (Greenland Sea) and the Bering Strait (Chukchi
608 Sea. The relation of landfast ice to the timing of break-up is discussed further in Section 4.
609 While the general trend towards earlier break-up noted above (Figure 6) is apparent at most of
610 the coastal locations, the magnitudes of the trends can differ between the coastal sites and the
611 broader MASIE regions. Figure 9 shows that the trend towards an earlier start of break-up is
612 stronger at the coastal location relative to the MASIE region at Churchill, Clyde River, Pevek
613 and Sabetta. Only at Tiksi is the negative trend weaker at the coastal site. In the other regions
614 the trends are nearly identical.

Deleted: 8

Deleted: (Bering Sea),

Deleted:). These locations are less prone to experience a buildup of landfast ice during the winter. The results imply that landfast ice plays a role in the timing of the start of breakup at coastal locations relative to the broader sector of the seasonal sea ice zone.

Deleted: processes by which

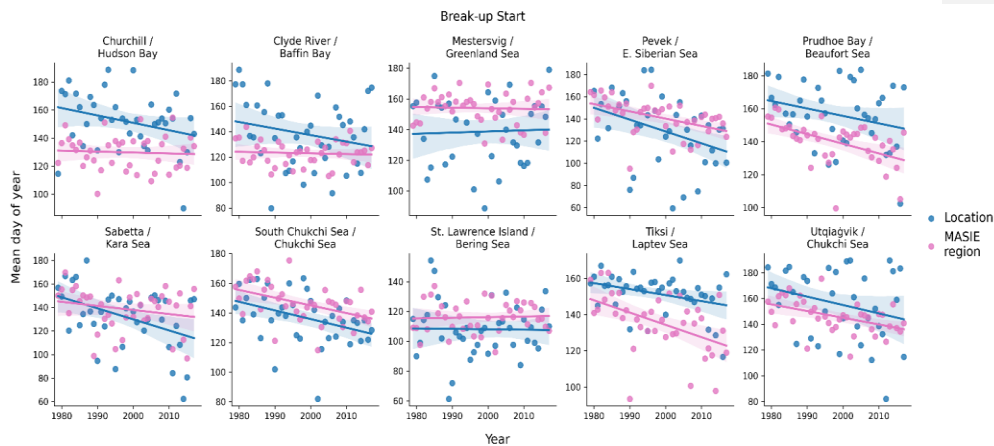
Deleted: affects

Deleted: are

Deleted: 5

Deleted: 8

Deleted:



630

631 Figure 9. Yearly values (1979-2018) of the break-up start dates (shown as day-of-the-year numbers)

Deleted: 8

632 for the coastal locations (blue) and the corresponding MASIE regions (pink). Date scales on y-axis vary

Deleted: purple

633 among panels in order to optimize display of data points. Linear regression lines are shown with the

634 same color coding. In each panel, the upper line of header identifies the coastal location and the lower

635 line identifies the MASIE region. All values are based on the modified J&E algorithms. Slopes and

636 their significance levels are listed in Tables S2 and S3.

637 The break-up end dates (Figure 10) show differences similar to those in Figure 9 in most, but

Deleted: 9

638 not all, cases. The break-up end date occurs later at Clyde River, Prudhoe and Utqiagvik

Deleted: 8

Deleted: earlier

639 relative to the MASIE regions, as is the case with the results in Figure 9. However, unlike the

Deleted: 8

640 break-up start date, the break-up end date also occurs later at Mestersvig than for the Greenland

Deleted: earlier

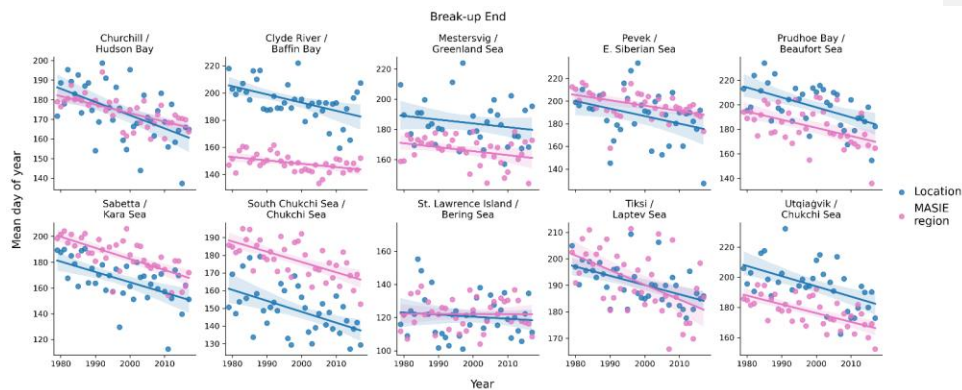
641 Sea MASIE region. The opposite relationship is found in the Kara Sea / Sabetta and the

642 Chukchi Sea (Bering Strait), where the MASIE region has the earlier break-up end date. The

643 temporal trends in the break-up end dates are generally similar for the coastal locations and

644 the MASIE regions, and there are no differences in sign. All coastal locations and all MASIE

645 regions show negative trends, i.e., trends toward earlier break-up end dates in recent decades.



653

654 Figure 10. Yearly values (1979-2018) of the break-up end dates (shown as day-of-the-year
 655 numbers) for the coastal locations (blue) and the corresponding MASIE regions (pink). Date
 656 scales on y-axis vary among panels in order to optimize display of data points. Linear
 657 regression lines are shown with the same color coding. In each panel, the upper line of header
 658 identifies the coastal location and the lower line identifies the MASIE region. All values are
 659 based on the modified J&E algorithms. Slopes and significance levels are listed in Tables S2
 660 and S3.

Deleted: 9

Deleted: purple

Deleted:

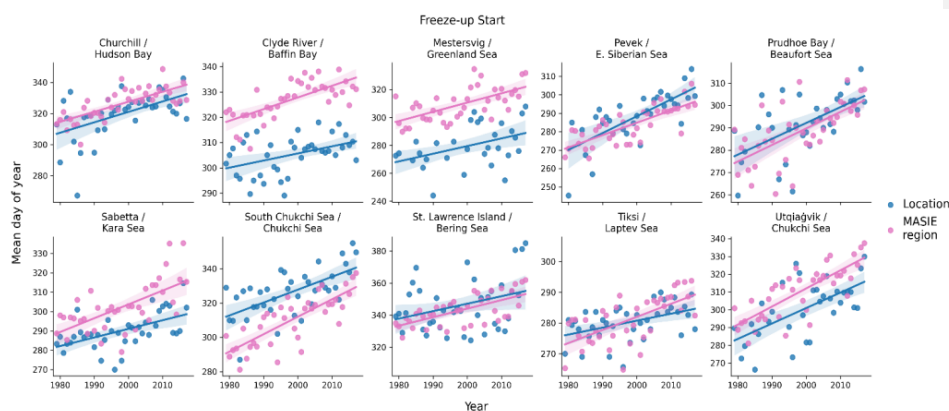
Deleted: their

661 The freeze-up start dates are compared in Figure 11. Several regions show large offsets, most
 662 notably Clyde River (Baffin Bay) and Mestersvig (Greenland Sea), where the start of freeze-
 663 up occurs earlier at the coast by several weeks. Both Baffin Bay and the Greenland Sea are
 664 large MASIE regions (Figure 2), favoring the delay of freeze-up start over a substantial
 665 portion of the seasonal sea ice zone within the respective MASIE regions. Freeze-up start
 666 dates are also earlier than offshore at several other coastal locations: Churchill, Sabetta and
 667 Utqiagvik. These are regions in which it is common for ice to form along the coast in autumn,
 668 with the ice edge advancing offshore to meet the expanding main ice pack as freeze-up

Formatted: Space After: 18 pt

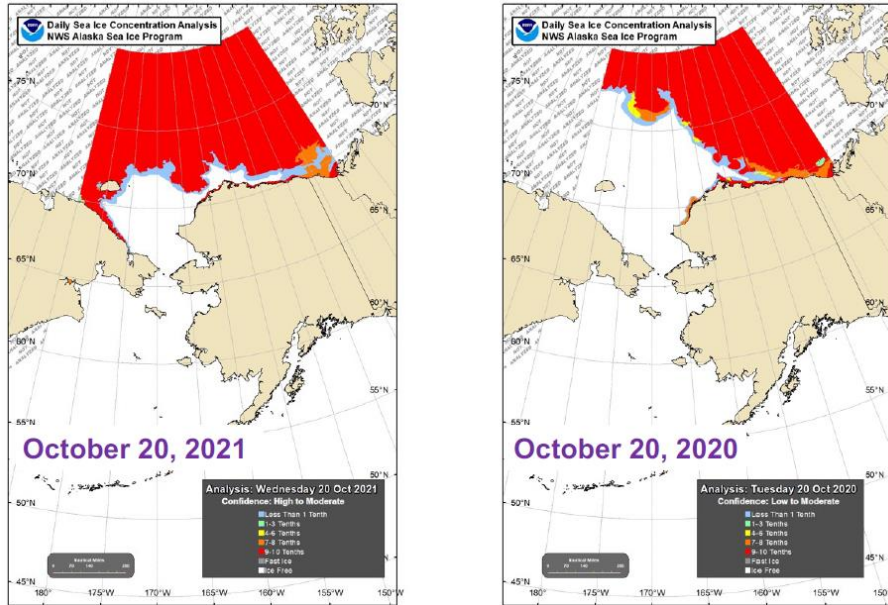
Deleted: 10

674 progresses. Figure 12 shows examples of this dual advance of the freeze-up “front” along the
 675 coasts of the East Siberian Sea in 2021 and the Beaufort Sea in 2020 and 2021. By contrast,
 676 the southern Chukchi Sea location has a later freeze-up date than the Chukchi MASIE region,
 677 largely because the southern Chukchi grid cells are located in an area of relatively warm
 678 inflowing currents from the Bering Sea and are in the southern portion of the Chukchi MASIE
 679 region. As with the break-up end dates, all coastal locations and MASIE regions show trends
 680 of the same sign. In this case, the trends are all positive, indicating a later start to freeze-up.



681
 682 Figure 11. Yearly values (1979-2018) of the freeze-up start dates (shown as day-of-the-year
 683 numbers) for the coastal locations (blue) and the corresponding MASIE regions (pink). Date
 684 scales on y-axis vary among panels in order to optimize display of data points. Linear
 685 regression lines are shown with the same color coding. In each panel, the upper line of header
 686 identifies the coastal location and the lower line lists the MASIE region. All values are based
 687 on the modified J&E algorithms. See Tables S2 and S3 for slopes and significance levels.

688



689

690 Figure 12. Sea ice coverage on October 20, 2021 (left panel) and October 20, 2020 (right
 691 panel). As indicated by legends in lower right of each panel, red denotes essentially complete
 692 ice coverage, while gray areas have low concentrations. Source: NWS Alaska Region Sea
 693 Ice Desk.

694

695 Finally, Figure 13 compares the freeze-up end dates for the ten coastal sites and their MASIE
 696 regions. The results are quite similar to those for the freeze-up start dates in Figure 11.

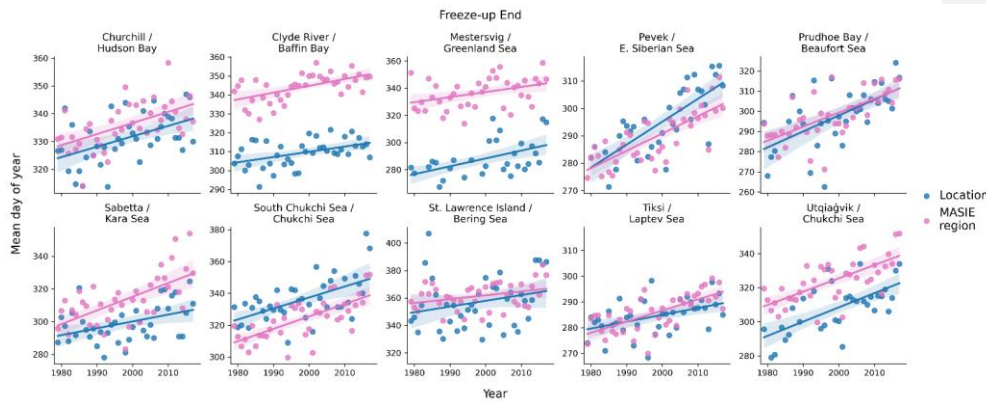
697 Relative to the MASIE regions as a whole, freeze-up ends earlier at both Canadian sites
 698 (Churchill and Clyde River), Mestersvig, Sabetta and Utqiagvik. Again, the differences are
 699 especially large (more than a month) at Clyde River and Mestersvig, both of which are in
 700 large MASIE regions as noted above. The southern Chukchi Sea and, to a lesser extent in

Formatted: Line spacing: Double

Deleted: 11

Deleted: 10

703 recent decades, Pevek (East Siberian Sea) show later freeze-ups near the coast than for the
 704 MASIE region. Once again, all trends are positive, pointing to a later end to freeze-up at
 705 coastal as well as offshore regions throughout the Arctic. The changes in the freeze-up dates
 706 over the 40-year period are especially large, exceeding one month, at Pevek (East Siberian
 707 Sea) and Prudhoe (Beaufort Sea). The changes are close to a month at Utqiaġvik (Chukchi
 708 Sea) and the Southern Chukchi Sea.



709

710 Figure 13. Yearly values (1979-2018) of the freeze-up dates (shown as day-of-the-year
 711 numbers) for the coastal locations (blue) and the corresponding MASIE regions (pink). Date
 712 scales on y-axis vary among panels in order to optimize display of data points. Linear
 713 regression lines are shown with the same color coding. In each panel, the upper line of header
 714 identifies the coastal location and the lower line identifies the MASIE region. All values are
 715 based on the modified J&E algorithms. Slopes and their significance levels are listed in Tables
 716 S2 and S3.

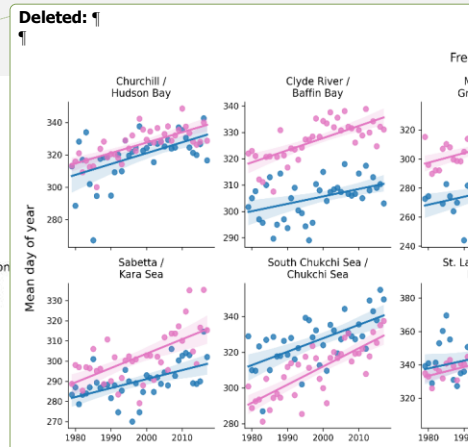


Figure 10. Yearly values (1979-2018) of the freeze-up start dates (shown as day-of-the-year numbers) for the coastal locations (blue) and the corresponding MASIE regions (pink). Date scales on y-axis vary among panels in order to optimize display of data points. Linear regression lines are shown with the same color coding. In each panel, the upper line of header identifies the coastal location and the lower line identifies the MASIE region. All values are based on the modified J&E algorithms. Slopes and their significance levels are listed in Tables S2 and S3.

Deleted: 11

Deleted: purple

732 In order to synthesize the information provided by the local indicators, we applied a factor
733 analysis to each of the four local indicators described in Section 2. For the local indicators,
734 each input matrix was 10 (locations) x 40 (years). For comparison, we also applied the factor
735 analysis to the corresponding regional sea ice areas from the MASIE database (National Snow
736 and Ice Data Center dataset G02135_v3.0-4). Because the Chukchi Sea is the MASIE region
737 for two of the local indicators (Chukchi Sea and Utqiagvik), the data matrix for the MASIE
738 regional factor analysis contained 9 (regions) x 40 (years) entries. We performed the MASIE
739 factors separately for middle months of the break-up and freeze-up seasons (June and
740 November, respectively).

741 In all cases, the first factor contains loadings of the same sign for all locations/regions and is
742 essentially a depiction of the temporal trends, which account for substantial percentages of the
743 variance. The second factor consists of loadings of both signs, corresponding to positive
744 departures from the mean at some locations and negative departures at others. Figure 14
745 illustrates this behavior for (a) the break-up start dates and (b) the freeze-up end dates. While
746 every one of the ten locations has a positive loading in Factor 1, the mixed signs of the Factor
747 2 loadings point to a regional clustering of the dates. For example, Figure 14a shows that the
748 northern coastal sites in the Pacific hemisphere from 90°E eastward to 90°W (Prudhoe Bay,
749 Utqiagvik, Tiksi, Pevek), have a component of break-up start date variability that is out of
750 phase with the locations in the western Atlantic/eastern Canada sector from 90°W eastward to
751 90°E (Mestersvig, Churchill, Clyde River).

752 The interpretation of Factor 1 as a trend mode is supported by Figure 15, which shows the
753 time series of the scores of Factor 1 for (a) the break-up start date and (b) freeze-up end dates.
754 The trends towards an earlier start of break-up and a later end of freeze-up are clearly evident.

Deleted: 12

Deleted: 12a

Deleted: (

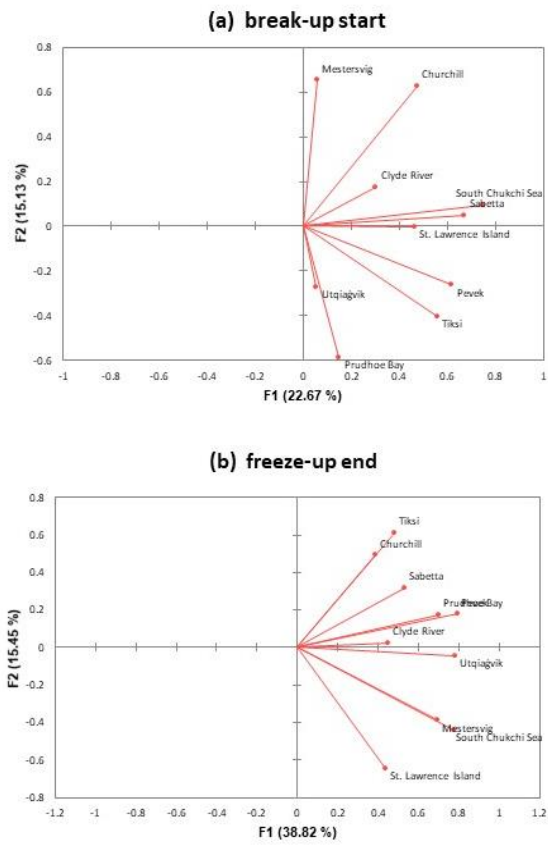
Deleted:)

Formatted: Space After: 0 pt

Deleted: 13

760 Figure 15 also illustrates the tendency for occasional “outlier” years to be followed by a
 761 recovery in the following year. These plots and those for the other local indicators show that
 762 these extreme excursions and recoveries are superimposed on the strong underlying trends,
 763 resulting in new extremes when the sign of an extreme year is the same as the sign of the
 764 underlying trend.

Deleted: 13



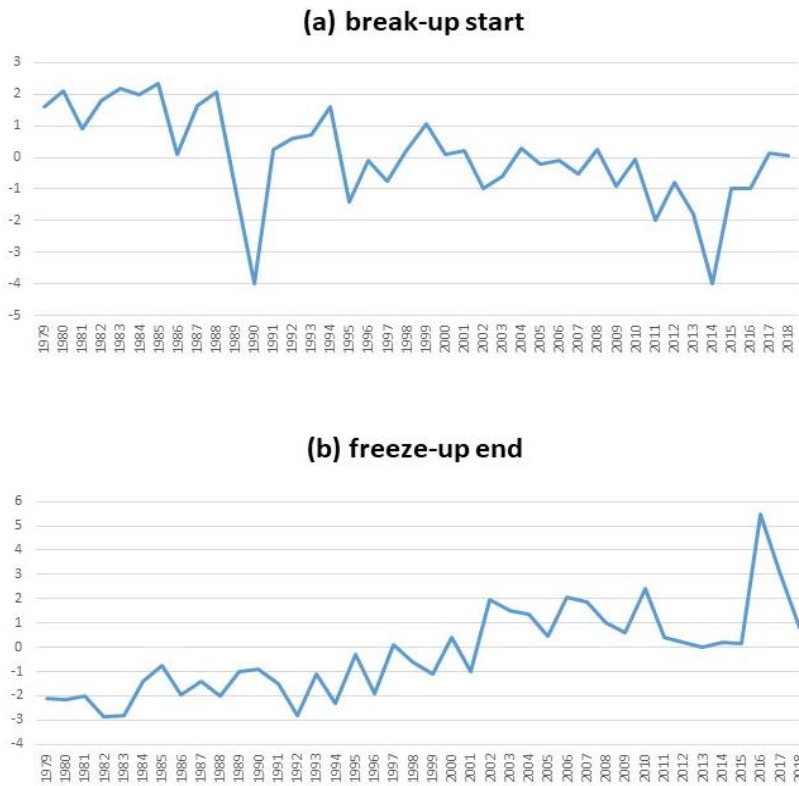
765

766 Figure 14. Loadings for Factor 1 (x-axis) and Factor 2 (y-axis) for (a) the start of break-up and (b)
 767 the end of freeze-up at the ten local coastal sites. Labels on vectors denote locations.

Formatted: Right: -0.31", Tab stops: 0", Left

Deleted: 12

Deleted: ¶



771

772 Figure 15. Scores (time series) for Factor 1 of (a) the start of break-up and (b) the end of
 773 freeze-up at the ten local coastal sites.

774 Table 4 shows that the first two factors explained more than half the variance for all local and
 775 MASIE indicators except the local break-up start date. The break-up start date is notable for
 776 the small percentages of variance explained by the first two factors. The implication is that
 777 local conditions play a relatively greater role in the timing of the start of break-up. These local
 778 factors can include landfast ice, inflow of water and heat from the adjacent land areas
 779 (including rivers), and possibly other effects related to local ocean currents or local weather

Formatted: Indent: Left: 0", First line: 0", Space After: 18 pt, Tab stops: 0", Left
 Deleted: 13
 Deleted: ¶

782 conditions. The freeze-up start date has the most spatial coherence in the trend mode (55.7%
783 of the explained variance). However, as shown by the last two lines of Table 4, the MASIE
784 regional ice areas have even greater percentages of variance explained by the first two factors.
785 In both the break-up and freeze-up seasons (June and November), the first two factors explain
786 more than 60% of the variance (vs. 37.8%-55.7% for the local indicators). Because the
787 variance of the ice concentrations in the MASIE regions is generally greater in the southern
788 compared to the northern portion of the region, factors for individual MASIE regions have
789 greater loadings in the south. However, this does not provide an obvious explanation for why
790 the percentage of variance explained by the first factor is greater for the MASIE indicators
791 than for the local indicators. These differences again point to the importance of local
792 conditions relative to the broader underlying trend in ice coverage, as Factor 1 (the trend)
793 accounts for most of the differences between the local and regional results in Table 4.

794

795 Table 4. Percentages of variance explained by Factors 1 and 2. Numbers in parentheses are
796 the contributions of the individual factors (Factor 1 + Factor 2).

797

798	Break-up start (local)	37.8%	(22.7% + 15.1%)
799	Break-up end (local)	50.9%	(37.6% + 13.3%)
800	Freeze-up start (local)	55.7%	(40.1% + 15.6%)
801	Freeze-up end (local)	54.3%	(38.8% + 15.5%)
802			
803	MASIE ice areas: June	60.9%	(47.1% + 13.8%)
804	MASIE ice areas: November	64.1%	(48.7% + 15.4%)

805

806 Finally, Figure 16 illustrates the tendency for tighter clustering in the regional indicators. For
807 both the June and November results, the clustering in Figure 16 is clearly more distinct than in
808 Figure 14, which is the corresponding figure for the local indicators. The clustering in Figure
809 16 is geographically coherent, e.g., the Pacific sector sites (Bering, Chukchi, East Siberian)
810 are in a distinct cluster for the June (break-up), while subclusters for November include the
811 Hudson and Baffin regions, the Kara and Laptev regions, and the Bering and Chukchi regions.
812 The results imply that underlying trends and spatially coherent patterns of forcing will be
813 more useful in explaining – and ultimately predicting – variations of regional sea ice cover.
814 However, diagnosis and prediction of local indicators will require a greater reliance on
815 additional information such as local geography and local knowledge, including information
816 from residents and other stakeholders who have had experience with break-up and freeze-up
817 of sea ice in the immediate area.

818

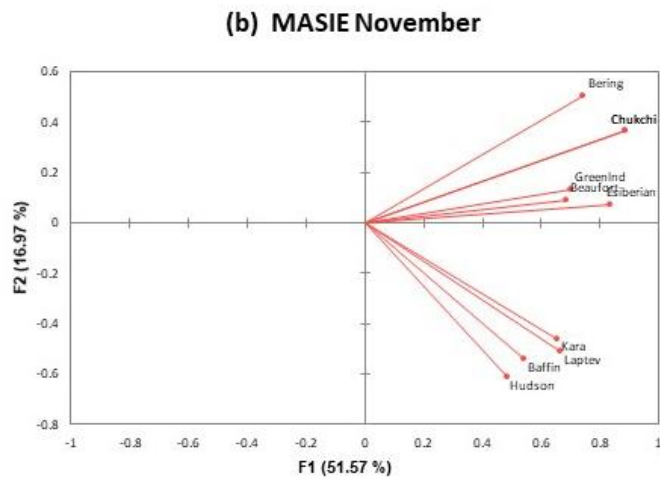
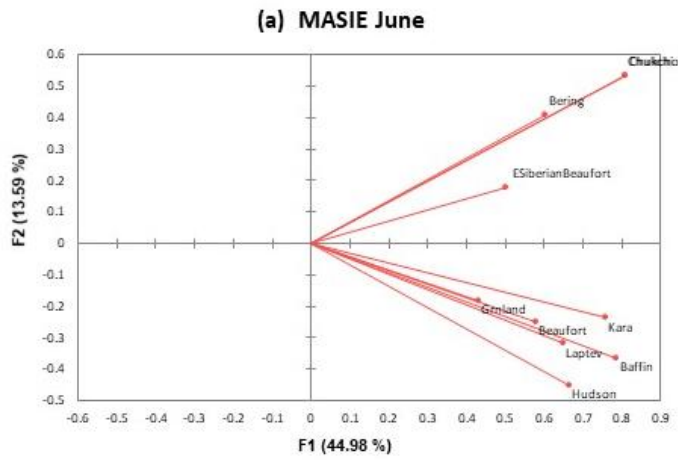
819

Deleted: 14

Deleted: 14

Deleted: 12

Deleted: 14



824

825 Figure 16. Loadings for Factor 1 (x-axis) and Factor 2 (y-axis) for the MASIE regional ice
 826 areas of (a) June and (b) November. Labels on vectors denote MASIE regions.

827

Deleted: 14

829 **4. Discussion**

830 The results presented in Section 3 point to a lengthening of the open water season as a result
831 of both an earlier break-up and a later freeze-up. The timing of break-up and freeze-up differs
832 between the coastal sites and the broader MASIE regions that are centered farther from shore
833 than the coastal grid cells. These differences can be related to the presence of landfast ice,
834 which characterizes the nearshore coastal waters to varying degrees at most of our coastal
835 sites (Figure 1).
836 Landfast ice generally persists longer than pack ice in the adjacent offshore in spring. This
837 contrast can be explained largely in terms of the stationary nature of the landfast ice cover,
838 with grounded pressure ridges and confinement by coastal barrier islands (e.g., in the Beaufort
839 and Kara Seas) locking the ice cover in place. Differences in ice thickness, with offshore sea
840 ice younger and hence thinner in areas of coastal polynyas with winter new-ice formation
841 (e.g., in the Chukchi, Beaufort and Laptev Seas) may also contribute to longer persistence of
842 landfast ice. Finally, with thermal decay of sea ice as a key break-up mode, the absorption of
843 solar shortwave energy in leads and openings in the offshore ice pack promotes thinning and
844 decay of the offshore ice relative to that of the landfast ice. The latter is mostly lacking such
845 areas of open water, rendering lateral melt and ocean-to-ice heat transfer from subsurface
846 ocean heat storage less effective (see also Petrich et al., 2012).

847 Table 5 summarizes the coastal-MASIE differences in break-up dates by grouping the sites
848 according to the role played by landfast ice. For several sites, the categorization of the fast ice
849 requires clarification. The Chukchi Sea location is a non-coastal site and therefore clearly
850 beyond the extent of landfast ice (Figure 1). The St. Lawrence Island grid cells used here are
851 considered to be unaffected by land fast ice because of their location southeast of the island,

Deleted:

Deleted: relates to the proximity to the coast

Deleted: In this section, we first place the trends obtained here in the context of past studies. We then address the distinct characteristics of the near-coastal waters by discussing landfast ice and its role in break-up and freeze-up, again drawing upon the published literature for context.
The lengthening of the open-water season in the Arctic has been well-documented (e.g., Stroeve et al., 2014; Stroeve and Notz, 2014).

Moved up [2]: The lengthening of the open-water season in the well-documented (e.g., Stroeve et al., 2014; Stroeve and Notz, 2018; Onarheim et al., 2018; Bliss and Anderson, 2018; Peng et al., 2019; Smith and Jahn, 2019). As a result, the percentage of the Arctic sea ice cover experiencing break-up and freeze-up (i.e., the percentage of the maximum ice cover that is seasonal) has increased from about 50% in 1980 to more than 70% in recent years (Druckemiller et al., 2019).

Deleted:

Deleted: Figure 15 shows the median and maximum extent of landfast ice during June for the period 1972-2007. Landfast ice is most extensive over shallow waters of the Siberian Seas and the Canadian Archipelago, although it can develop in the general vicinity of all of our sites (Fig. 1), with the exception of the offshore location in the Chukchi Sea. Given its widespread presence at the coastal sites in the Arctic, landfast ice a key feature in our

Moved up [3]: Figure 15 shows the median and maximum extent of landfast ice during June for the period 1972-2007. Landfast ice is most extensive over shallow waters of the Siberian Seas and the Canadian Archipelago, although it can develop in the general vicinity of all of our sites (Fig. 1), with the exception of the offshore location in the Chukchi Sea. Given its widespread presence at the coastal sites in the Arctic, landfast ice a key feature in our



Moved up [4]:

Formatted: Normal (Web), Space After: 18 pt

981 as described in Section 2. The grid cells representing the Mestersvig region are located in the
 982 coastal Greenland Sea, just outside of King Oscar Fjord. This region experiences dynamic ice
 983 conditions with a comparatively short landfast ice season and a narrower landfast ice belt,
 984 with ocean swell and ice pack interaction constraining extent and duration of the landfast ice
 985 cover (Wadhams, 1981). For this reason, Mestersvig is listed below the other sites affected by
 986 landfast ice in Table 5. With these caveats, it apparent from Table 5 that there is a general
 987 tendency for later break-up (both the start and end dates) at locations affected by landfast ice.
 988 The delay of the break-up ranges from about 5 to 40 days. Exceptions are Pevek and Sabetta,
 989 where local freshwater inflows from streams and snowmelt may contribute to earlier break-
 990 ups relative to the broader MASIE regions – a hypothesis that should be tested in future
 991 research. There is no clear signal of earlier or later coastal break-up at Mestersvig and St.
 992 Lawrence Island, where fast ice is not a major contributor to the timing of break-up. The
 993 earlier local break-up at the Chukchi site is primarily a function of its location in the southern
 994 portion of the Chukchi MASIE region.

995 Table 5. Summary of landfast ice presence at each coastal site and timing of break-up at the
 996 site relative to break-up in corresponding MASIE region (Figures 10 and 11).

	<u>Landfast ice?</u>	<u>Break-up start (vs. MASIE)</u>	<u>Break-up end (vs. MASIE)</u>
998 Churchill	yes	later (~20 days)	similar
999 Clyde River	yes	later (~10 days)	later (~40 days)
1000 Prudhoe Bay	yes	later (~15 days)	later (~15 days)
1001 Utqiagvik	yes	later (~10 days)	later (~15 days)

Formatted: Underline

Formatted: Underline

1002	Tiksi	yes	later (~15 days)	similar
1003	Pevek	yes	earlier (~5 days)	earlier (~5 days)
1004	Sabetta	yes	similar	earlier (~15 days)
1005	Mestersvig	(yes)	earlier (~20 days)	later (~15 days)
1006	St. Lawrence I.	no	earlier (~5 days)	similar
1007	Chukchi Sea	no	earlier (~10 days)	earlier (~35 days)

1008

1009 In the autumn, water in the shallow coastal areas cools more rapidly to the freezing point
1010 because there is less stored heat below the surface. Coastal waters can also be fresher than
1011 offshore waters because of terrestrial runoff that freshens the nearshore areas during the warm
1012 season. Under such conditions both a higher freezing point and reduction of convective
1013 overturning promote earlier freeze-up (Dmitrenko et al., 1999). As a result, the autumn freeze-
1014 up often proceeds outward from the coast as well as shoreward from the main pack ice (Figure
1015 12). However, onset of freeze-up – and depending on the geographic setting and offshore
1016 ocean and atmosphere conditions potentially also end of freeze-up – do not correspond with
1017 onset of landfast ice formation. In the Chukchi and Beaufort Sea, first appearance of landfast
1018 ice may lag freeze onset by a couple of weeks to three months (Mahoney et al., 2014). In more
1019 sheltered and less dynamic environments such as the Laptev Sea, inshore landfast ice typically
1020 does not form for another couple of weeks after onset of freeze-up and generally takes more
1021 than a month to extend further offshore (Selyuzhenok et al., 2015). Hence, freeze-up

Deleted: For coastal sites situated partly or wholly within a landfast ice zone, the breakup dates described in Section 3 are highly dependent on the break-up of the landfast ice. Petrich et al. (2012) describe two dominant break-up modes for landfast ice. Dynamic or mechanical break-up occurs when the action of the wind, ocean swell or currents, and variations in sealevel height promote weakening of the ice cover, detachment from the seafloor and advection of the ice away from the coast. Thermal breakup results from surface and bottom ablation and internal melt, aided further by formation of surface melt ponds. Dispersion is not required for thermal breakup. As noted by Petrich et al. (2012), the mode of ice breakup is often determined by the extent of grounded pressure ridges.¶

Deleted: Thomson et al., 2022, their Fig. 4

1036 variability and trends reported in this study are seen as largely independent of landfast ice
1037 processes.

1038 Conversely, timing of freeze-up does impact the seasonal evolution of landfast ice. Mahoney
1039 et al. (2007) discuss mean climatology of annual landfast ice from 1996-2004, including
1040 analyses of the maximum, minimum and mean extents. Notable for the results presented in
1041 the present study is Mahoney et al.'s finding of a reduced presence of landfast ice in Beaufort-
1042 Chukchi region, due to later formation and earlier breakup. In a follow-up study, Mahoney et
1043 al. (2014) addressed the geographical variability of break-up and freeze-up, especially as it
1044 relates to landfast ice. Their results show that landfast ice in the central and western Beaufort
1045 Sea forms earlier, breaks up later, occupies deeper water and extends further from shore than
1046 that in the Chukchi Sea. These differences are partially due to the orientation of the coastline
1047 relative to the prevailing easterly winds, which can more readily advect ice away from the
1048 southwest-northeast oriented coastline of the Chukchi Sea. Hosekova et al. (2021) examined
1049 landfast ice along the northern Alaska coast in the context of the buffering of the coastline
1050 from wave activity. They found that the wave attenuation by landfast ice was weaker in
1051 autumn than in spring because of the lower ice thickness in autumn compared to spring.
1052 However, the importance of waves for breakup is somewhat limited because it typically
1053 requires large fetch with does not develop until later in the summer and fall, well past the end
1054 of break-up season.

1055 Yu et al. (2014) showed that landfast ice has large interannual variations, which imply large
1056 variations in break-up and freeze-up. Superimposed on these variations were notable trends in
1057 landfast ice during Yu et al's study period, 1976-2007. More specifically, the duration of
1058 landfast ice was found to have shortened in the Chukchi, East Siberian and Laptev Seas,

1059 primarily as a result of a slower offshore expansion of landfast ice during the autumn and
1060 early sinter since 1990. Our coastal sites in these sectors (Utqiagvik, Pevek and Tiksi) show
1061 notable trends toward earlier break-up and later freeze-up, consistent with Yu et al.'s (2014)
1062 trends in landfast ice.

1063
1064 Cooley et al. (2020) examined the sensitivity of landfast ice break-up at the community level
1065 in the Canadian Arctic and western Greenland to temperature variations and trends based on
1066 analysis of visible satellite imagery. Our analysis provides a longer reference period (40 years
1067 vs. 19 years) and a broader geographical context for the work by Cooley and collaborators.
1068 Cooley et al. (2020) also used the relationships between air temperature and landfast ice
1069 break-up date, together with projected changes in air temperature from a set of eight CMIP5
1070 global climate models, to project future changes in the breakup dates. Specifically, we note
1071 that the trends projected for the remainder of the century in Cooley et al. (2020) are in many
1072 instances less pronounced (in days/decade shift in breakup) than those identified here. For
1073 example, for Clyde River Cooley et al. project a shift in breakup to an earlier date by 23 days
1074 by the year 2099 as compared to changes of a similar magnitude but over a much shorter time
1075 period examined here (Fig. 9 and 10). For Clyde River, the comparison between trends in the
1076 local break-up timing compared to that for the broader region (Baffin Bay) also reveals that
1077 the regional trends are much less pronounced than those at the local scale (Fig. 9 and 10).
1078 Furthermore, the two westernmost communities examined by Cooley et al. (2020),
1079 Tuktoyaktuk and Paulatuk (Eastern Beaufort Sea), were projected to see earlier landfast ice
1080 break-up onset of 5 days and 11 days, respectively, by 2099. The data compiled here for
1081 Prudhoe Bay and the Beaufort Sea indicate a substantially larger shift towards earlier dates by
1082 more than 5 days *per decade* (Fig. 9 and 10).

Deleted: 8

Deleted: 9

Deleted: 8

Deleted: 9

Deleted: 8

Deleted: 9

1089 One other study that addressed future changes of sea ice duration in the Pacific sector of the
1090 Arctic is Wang et al.'s (2018) evaluation mid-21st-century projections based on sea ice
1091 concentrations simulated by seven CMIP5 global climate models. However, Wang et al.'s
1092 evaluations were for the broader offshore areas of the East Siberian, Chukchi and Beaufort
1093 Seas rather than for immediate coastal areas, as global climate models generally do not
1094 include landfast ice. Pan-Arctic models that simulated landfast ice parameterized
1095 thermodynamically without addressing its mobility had significant problems in forecasting
1096 coastal ice thickness, especially during freeze-up in September and October (Johnson et al.,
1097 2012). The projected increases in ice-free season length over the 2015-2044 period were
1098 found to vary from about 20 days in the Bering Strait region to up to 60 days in
1099 the offshore areas of the East Siberian, Chukchi and Beaufort Seas. While these changes are
1100 for offshore areas, they are larger than those projected for coastal areas by late century in the
1101 study of Cooley et al. (2020).

1102 **5. Conclusion**

1103 The primary objective of this study was to use the locally-based metrics to construct
1104 indicators of break-up and freeze-up at near-coastal locations in which sea ice has high
1105 stakeholder relevance. A set of ten coastal locations distributed around the Arctic were
1106 selected for this purpose. The sea ice indicators used here are based on local ice climatologies
1107 informed by community ice use (Johnson and Eicken, 2016; Eicken et al., 2014) rather than
1108 prescribed "universal" thresholds of ice concentration (e.g., 15%, 80%) used in other recent
1109 studies of sea ice break-up and freeze-up.

1110 The trends and interannual variations of the local indicators of break-up and freeze-up at the
1111 ten nearshore are similar to the trends and variations of corresponding indicators for broader
1112 offshore regions, but the site-specific indicators often differ from the regional indicators by
1113 several days to several weeks. Relative to indicators for broader adjacent seas, the coastal
1114 indicators show later break-up at sites known to have extensive landfast ice, whose break-up
1115 typically lags retreat of the adjacent, thinner drifting ice. The coastal indicators also show an
1116 earlier freeze-up at some sites in comparison with freeze-up for broader offshore regions,
1117 likely tied to earlier freezing of shallow water regions and areas affected by freshwater input
1118 from nearby streams and rivers. However, the trends towards earlier break-up and later freeze-
1119 up are unmistakable over the post-1979 period at nearly all the coastal sites and their
1120 corresponding regional seas.

1121 The coastal indicators of the seasonal ice cycle for this study are based on Alaskan ice users.
1122 However, ice uses and ice hazards in this region, as reflected in the definition of key seasonal
1123 indicators, align with those of other coastal regions in the Arctic. Specifically, the
1124 commonalities between coastal populations using the sea ice cover (both drifting and landfast)
1125 as a platform for a range of activities, and to whom sea ice poses a hazard for boating and
1126 marine vessel traffic, justify the approach taken in this study to extrapolate from the Alaskan
1127 Arctic (with a range of ice conditions representative of the broader Arctic) to the pan-Arctic
1128 scale.

1129 The differences between the coastal and offshore regional indicators matter greatly to local
1130 users whose harvesting of coastal resources and Indigenous culture are closely tied to the
1131 timing of key events in the seasonal ice cycle (Huntington et al., 2021; Eicken et al., 2014).
1132 These differences also matter from the perspective of maritime activities, where access to

Deleted: with

Formatted: Space After: 18 pt

1134 coastal locations for destination traffic is a key factor (Brigham, 2017). These offsets vary
1135 considerably by region. In light of these findings, we view locally as well as regionally
1136 defined measures of sea-ice break-up and freeze-up as a key set of indicators linking pan-
1137 Arctic or global indicators such as sea-ice extent or volume to local and regional uses of sea
1138 ice, with the potential to inform community-scale adaptation and response.

Deleted: ¶

1139 **Acknowledgments**

1140 This work was supported by the Climate Program Office of the National Oceanic and
1141 Atmospheric Administration through Grant NA17OAR431060. Additional funding was
1142 provided by the Interdisciplinary Research for Arctic Coastal Environments (InterFACE)
1143 project through the U.S. Department of Energy, Office of Science, Biological and
1144 Environmental Research RGMA program.

Formatted: Space After: 18 pt

1145 **Data Availability**

1146 The daily grids of passive-microwave-derived sea ice concentrations are available from the
1147 National Snow and Ice Data Center as dataset NSIDC-0051, available at
1148 <https://nsidc.org/data/nsidc-0051>. Lists of the indicator dates for the coastal sites and the
1149 MASIE regions are available from the author on request.

Formatted: Space After: 18 pt

Deleted: ¶

1150 **Author contributions**

1151 JEW served the principal investigator for the study, led the drafting of the manuscript, and
1152 performed the factor analysis described in Section 3. HE supervised the implementation of
1153 the revised indicators for the coastal sites and the MASIE regions, and drafted parts of the
1154 text. KR performed the indicator calculations, produced Figures 1-11, and assisted in the

Formatted: Right: 0", Space After: 18 pt, Line spacing: Double

1158 preparation of the manuscript. MJ designed the original indicators, participated in the

1159 modification of the indicators, and contributed to the revision of the manuscript.

Deleted: ¶

1160 Competing interests

1161 The authors declare that they have no conflict of interest.

Formatted: Right: -0.69", Space After: 24 pt

Deleted: ¶

1162 References

1163 AMAP: Adaptation Actions for a Changing Arctic: Perspectives from the Baffin Bay/Davis
1164 Strait Region. Arctic Monitoring and Assessment Programme (AMAP), Oslo, Norway. xvi +
1165 354 pp, <https://www.amap.no/documents/download/3015/inline>, 2018.

1166 AMAP: Snow, water, ice and permafrost in the Arctic (SWIPA) 2017, Arctic Monitoring and
1167 Assessment Programme (AMAP), Oslo, Norway, xiv + 269 pp. 2017.

1168 Bliss, A.C., and Anderson, M.R.: Arctic sea ice melt onset and timing from passive
1169 microwave- and surface air temperature-based methods, *J. Geophys. Res.*, 123, 9063-9080,
1170 <https://doi.org/10.1029/2018JD028676>, 2018.

1171 Bliss, A.C., Steele, M., Peng, G., Meier, W.M., and Dickinson, S: Regional variability of
1172 Arctic sea ice seasonal climate change indicators from a passive microwave climate data
1173 record, *Environ. Res. Lett.*, 14, 045003, <https://doi.org/10.1088/1748-9326/aafb84>, 2019.

1174 Box, J.E., and 19 coauthors: Key indicators of Arctic climate change: 1971–2017, *Environ.*
1175 *Res. Lett.*, 14(4), 045010, <https://doi.org/10.1088/1748-9326/aafc1b>, 2019.

1176 ,
1177 Brigham, L.W.: The changing maritime Arctic and new marine operations. In: Beckman, R.
1178 C., Henriksen, T., Dalaker Kraabel, K., Molenaar, E. J., and Roach, J. A. (eds.): *Governance*
1179 *of Arctic shipping* (pp. 1-23), Brill Nijhoff, 2017.

1180 Cavalieri, D.J., Gloersen, P., and Campbell, W.J.: Determination of sea ice parameters with
1181 the NIMBUS-7 SMMR, *J. Geophys. Res.*, 89(D4): 5355-5369,
1182 <https://doi.org/10.1029/JD089iD04p05355>, 1984.

1183 Cooley, S.W., Ryan, J.C., Smith, L.C., Horvat, C., Pearson, B., Dale, B. and Lynch, A.H.:
1184 Coldest Canadian Arctic communities face greatest reductions in shorefast sea ice. *Nature*
1185 *Climate Change*, 10(6), pp.533-538.
1186 <https://www.nature.com/articles/s41558-020-0757-5>, 2020.

1187
1188 Dammann, D.O., Eicken, H., Mahoney, A.R., Meyer, F.J. and Betcher, S: Assessing sea ice
1189 trafficability in a changing Arctic. *Arctic*, 71(1), 59-75, <https://doi.org/10.14430/arctic4701>,
1190 2018.

Deleted: ¶

Comiso, J. C: Characteristics of Arctic Winter Sea Ice from Satellite
Multispectral Microwave Observations, *J. Geophys. Res.*, 91(C1),
5C0766, 975-994, 1986¶

1204 Deser, C., Walsh, J.E., and Timlin, M.S.: Arctic sea ice variability in the context of recent
1205 atmospheric circulation trends, *J. Climate*, 13, 617-633, [https://doi.org/10.1175/1520-0442\(2000\)013<0617:ASIVIT>2.0.CO;2](https://doi.org/10.1175/1520-0442(2000)013<0617:ASIVIT>2.0.CO;2), 2000.

1207 Druckenmiller, M.L. et al.: The Arctic. *Bull. Amer. Meteor. Soc.*, 102, S263-S316,
1208 <https://doi.org/10.1175/BAMS-D-21-0086.1>, 2021.

1209 Eicken, H., Kaufman, M., Krupnik, I., Pulsifer, P., Apangalook, L., Apangalook, P., Weyapuk
1210 Jr, W., and Leavitt, J.: A framework and database for community sea ice observations in a
1211 changing Arctic: An Alaskan prototype for multiple users, *Polar Geogr.*, 37(1), 5-27,
1212 <http://dx.doi.org/10.1080/1088937X.2013.873090>, 2014.

1213
1214 Fang, A., and Wallace, J. M.: Arctic sea ice variability on a timescale of weeks in relation to
1215 atmospheric forcing, *J. Climate*, 7, 1897-1914, [https://doi.org/10.1175/1520-0442\(1994\)007<1897:ASIVOA>2.0.CO;2](https://doi.org/10.1175/1520-0442(1994)007<1897:ASIVOA>2.0.CO;2), 1994. .

1217
1218 Fu, D., Liu, B., Yu, G., Huang, H., and Qu, L: Multiscale variations in Arctic sea ice motion
1219 and links to atmospheric and oceanic conditions, *The Cryosphere*, 15, 3797-3811,
1220 <https://doi.org/10.5194/tc-15-3797-2021>, 2021.

1221
1222 Hosekova, L., Eidam, E., Panteleev, G., Rainville, L., Rogers, W.E., and Thomson, J.:
1223 Landfast ice and coastal wave exposure in northern Alaska. *Geophys. Res. Lett.*, 48(22),
1224 e2021GL095103, <https://doi.org/10.1029/2021GL095103>, 2021.

1225
1226 Huntington, H. P., Raymond-Yakoubian, J., Noongwook, G., Naylor, N., Harris, C.,
1227 Harcharek, Q. and Adams, B.: “We never get stuck”: A collaborative analysis of change and
1228 coastal community subsistence practices in the northern Bering and Chukchi Seas,
1229 *Alaska, Arctic*, 74(2), 113-126, 2021.

1230
1231 IPCC: Climate Change 2021: The Physical Science Basis. Contribution of Working Group I
1232 to the Sixth Assessment Report of the Intergovernmental Panel on Climate Change [Masson-
1233 Delmotte, V., Zhai, P., Pirani, A., Connors, S. L., Péan, C., Berger, S., Caud, N., Chen, Y.,
1234 Goldfarb, L., Gomis, M. I., Huang, M., Leitzell, K. Lonnoy, E., Matthews, J. B. R., Maycock,
1235 T. K., Waterfield, Y., Yelekçi, O., Yu, R., and Zho, B. (eds.)]. Intergovernmental Panel on
1236 Climate Change, Cambridge University Press.
1237 <https://www.bing.com/search?FORM=AFSCVO&PC=AFSC&q=IPCC+AR6+Working+Group+1+report>, 2022.

1238
1239
1240 Johnson, M., and Eicken, H.: Estimating Arctic sea-ice freeze-up and break-up from the
1241 satellite record: A comparison of different approaches in the Chukchi and Beaufort Seas,
1242 *Elementa: Science of the Anthropocene*, 4, 000124, doi:10.12952/journal.elementa.000124,
1243 2016.

1244
1245 Johnson, M., et al.: Evaluation of Arctic sea ice thickness simulated by Arctic Ocean Model
1246 Intercomparison Project models, *J. Geophys. Res.*, 117, C00D13, doi:10.1029/2011JC007257,
1247 2012

1248

1249 Kapsch, M.L., Eicken, H., and Robards, M.: Sea ice distribution and ice use by indigenous
1250 walrus hunters on St. Lawrence Island, Alaska. In SIKU: Knowing Our Ice (Krupnik, I.,
1251 Aporta, C., Gearheard, S., Laidler, G. J., and Lielsen Holm, L., Eds.), 115-144, Springer,
1252 Dordrecht, 2010.
1253
1254 Krupnik, I., Apangalook, L., and Apangalook, P: "It's cold, but not cold enough": Observing
1255 ice and climate change in Gambell, Alaska, in IPY 2007-2008 and beyond. In SIKU:
1256 Knowing Our Ice (Krupnik, I., Aporta, C., Gearheard, S., Laidler, G. J., and Lielsen Holm, L.,
1257 Eds.), 81-114, Springer, Dordrecht, 2010.
1258
1259 Mahoney, A.R., Eicken H., Gaylord A.G., and Gens R.: Landfast sea ice extent in the
1260 Chukchi and Beaufort Seas: The annual cycle and decadal variability. *Cold Reg. Sci.*
1261 *Technol.*, 103, 41–56. doi: 10.1016/j.coldregions.2014.03.0033, 2014..
1262
1263 Mahoney, A.R., Eicken, H., Gaylord, A.G., and Shapiro, L: Alaska landfast sea ice: Links
1264 with bathymetry and atmospheric circulation, *J. Geophys. Res.*, 112, C02001,
1265 doi:10.1029/2006JC003559, 2007.
1266
1267 Markus, T., Stroeve J. C., and Miller, J: Recent changes in Arctic sea ice melt onset, freezeup
1268 and melt season length, *J. Geophys. Res. (Oceans)*, 114, 1-14,
1269 <https://doi.org/10.1029/2009JC005436>, 2009.
1270
1271 Meier, W., Fetterer, F., Savoie, M., Mallory, S. Duerr, R., and Stroeve, J.: NOAA/NSIDC
1272 Climate Data Record of Passive Microwave Sea Ice Concentration, Version 3 (Boulder,
1273 Colorado USA; National Snow and Ice Data Center), <https://doi.org/10.7265/N59P2ZTG>,
1274 [Accessed 16 January 2022, 2017].
1275
1276 Noongwook, G.: Native Village of Savoonga, Native Village of Gambell. In Huntington,
1277 H.F., and George, J.C.: Traditional knowledge of the bowhead whale (*Balaena mysticetus*)
1278 around St. Lawrence Island Alaska, 47-54, 2007.
1279
1280 Onarheim, I.H., Eldevik, T., Smedsrud, L.H., and Stroeve, J.C.: Seasonal and regional
1281 manifestations of Arctic sea ice loss, *J. Climate*, 31, 4917-4932, [https://doi.org/10.1175/JCLI-](https://doi.org/10.1175/JCLI-D-17-0427.1)
1282 [D-17-0427.1](https://doi.org/10.1175/JCLI-D-17-0427.1), 2018.
1283
1284 Peng, G., Steele, M., Bliss, A. C., Meier, W. N., and Dickinson, S: Temporal means and
1285 variability of Arctic sea ice melt and freeze season climate indicators using a satellite climate
1286 data record, *Remote Sensing*, 10, 1328, <https://doi.org/10.3390/rs10091328>, 2018.
1287
1288 Petrich, C., Eicken, H., Zhang, J., Krieger, J., Fukamachi, Y., and Ohshima, K.J.: Coastal
1289 landfast sea ice decay and breakup in northern Alaska: Key processes and seasonal prediction,
1290 *J. Geophys. Res.*, 117, C02003, doi:10.1029/2011JC007339, 2012.
1291
1292 Selyuzhenok, V., Krumpfen, T., Mahoney, A., Janout, M., and Gerdes, R.: Seasonal and
1293 interannual variability of fast ice extent in the southeastern Laptev Sea between 1999 and
1294 2013, *J. Geophys. Res. Oceans*, 120, 7791–7806, doi:10.1002/2015JC011135, 2015.

1295
1296 Smith, A., and Jahn, A.: Definition differences and internal variability affect the simulated
1297 Arctic sea ice melt season, *The Cryosphere*, 12, 1-20, <https://doi.org/10.5194/tc-13-1-2019>,
1298 2019.
1299
1300 Serreze, M.C., Crawford, A.D., Stroeve, J.C., Barrett, A.P. and Woodgate, R.A.: Variability,
1301 trends, and predictability of seasonal sea ice retreat and advance in the Chukchi Sea. *J.*
1302 *Geophys. Res. (Oceans)*, 127, 7308–7325, 2016.
1303
1304 Stammerjohn, S., Massom, R., Rind, D. and Martinson, D.: Regions of rapid sea ice change:
1305 an inter-hemispheric seasonal comparison. *Geophys. Res. Lett.* 39, L06501, 2017.
1306
1307 Stroeve, J.C., Crawford, A.D. and Stammerjohn, S.: Using timing of ice retreat to predict
1308 timing of fall freeze-up in the Arctic. *Geophys. Res. Lett.* 43, 6332–6340, 2016.
1309
1310 Stroeve, J.C., Markus, T., Boisvert, L., Miller, J., and Barrett, A.: Changes in Arctic melt
1311 season and implications for sea ice loss. *Geophys. Res. Lett.*, 41, 1216-1225,
1312 <https://doi.org/10.1002/2013GL058951>, 2014.
1313
1314 Stroeve, J., and Notz, D.: Changing state of Arctic sea ice across all seasons. *Env. Res. Lett.*,
1315 13, 102001, <https://doi.org/10.1088/1748-9326/aade56>, 2018.
1316
1317 Thomson, J., Smith, M., Drushka, K. and Lee, C.: Air-ice-ocean interactions and the delay of
1318 autumn freeze-up in the western Arctic Ocean. *Oceanography*,
1319 <https://doi.org/10.5670/oceanog.22.124>, 2022.
1320
1321 USGCRP: Climate Science Special Report: Fourth National Climate Assessment, Volume I
1322 (Wuebbles, D.J., Fahey, D.W., Hibbard, K.A., Dokken, D.J., Stewart, B.C., and Maycock,
1323 T.K.[eds.]). U.S. Global Change Research Program, Washington, DC, USA, 470 pp., doi:
1324 10.7930/J0J964J6, 2017

1325 [Wadhams, P.: The ice cover in the Greenland and Norwegian Seas. *Reviews of Geophysics*](#)
1326 [and *Space Physics*, 19\(3\), 345–93, doi: 10.1029/RG019i003_1981.](#)

1327 Wang, M., Yang, Q., Overland, J.E., and Stabeno, P.: Sea-ice cover timing in the Pacific
1328 Arctic: The present and projections to mid-century by selected CMIP5 models. *Deep Sea*
1329 *Research Part II: Topical Studies in Oceanography*, 152, 22-34,
1330 <https://www.sciencedirect.com/science/article/pii/S0967064516302132>, 2018
1331
1332 Walsh, J. E., and Johnson, C. M.: Interannual atmospheric variability and associated
1333 fluctuations in Arctic sea ice extent, *J. Geophys. Res.*, 84, 6915–6928,
1334 <https://doi.org/10.1029/JC084iC11p06915>, 1979.

1335 Yu, Y, Stern, H., Fowler, C., Fetterer, F., and Maslanik. J.: Interannual variability of Arctic
1336 landfast ice between 1976 and 2007. *J. Climate*, Vol. 27, 227-243, doi: [10.1175/JCLI-D-13-](https://doi.org/10.1175/JCLI-D-13-00178.1)
1337 [00178.1](https://doi.org/10.1175/JCLI-D-13-00178.1), 2014.

Deleted: ¶

Formatted: doi-p, Line spacing: single

Formatted: No underline

Formatted: Space After: 6 pt, Line spacing: single, Tab stops: 6.5", Right

Deleted: ¶

1341 **Supplementary material**

1342

1343 Table S1. Dates (Julian day numbers) corresponding to the modal values (peaks) of the
 1344 distributions in Figure 4. (Insufficient number of years met Bliss criteria in
 1345 Central Arctic).

1346

	Break-up		Break-up		Freeze-up		Freeze-up	
	Start		end		start		end	
	J&E	Bliss	J&E	Bliss	J&E	Bliss	J&R	Bliss
1347								
1348								
1349								
1350								
1351	Beaufort Sea	145 187	167 208		292 287		296 279	
1352	Chukchi Sea	147 177	181 202		315 312		325 302	
1353	E. Sibarian Sea	150 182	195 207		281 293		280 294	
1354	Laptev Sea	140 192	188 207		280 271		285 279	
1355	Kara Sea	145 193	190 209		304 299		307 296	
1356	Barents Sea	146 164	152 186		315 297		328 302	
1357	Greenland Sea	150 177	162 207		308 290		342 280	
1358	Baffin Bay	121 152	149 186		331 311		346 324	
1359	Canadian Arctic	147 208	190 207		279 274		298 275	
1360	Hudson Bay	139 159	177 198		322 317		326 325	
1361	Central Arctic	199	200		306		310	
1362	Bering Sea	110 123	123 142		343 337		362 349	

1363

1364

1365

1366

1367

1368

1369

1370

1371 Table S2. Slopes (least-squares linear regression lines) of the MASIE regions in Figures 5-6
 1372 and 8-11. Also shown are the explained variances (r^2 values of the trend lines and their levels
 1373 of statistical significance.

1374

Region	Indicator Group	Indicator	Slope (days yr ⁻¹)	r ²	significance level
Baffin Bay	Bliss	Day of Advance	0.4	0.57	< 0.01**
Baffin Bay	Bliss	Day of Closing	0.4	0.52	< 0.01**
Baffin Bay	Bliss	Day of Opening	-0.5	-0.74	< 0.01**
Baffin Bay	Bliss	Day of Retreat	-0.7	-0.77	< 0.01**
Baffin Bay	J&E	Break-up End	-0.2	-0.44	< 0.01**
Baffin Bay	J&E	Break-up Start	-0.1	-0.07	0.67
Baffin Bay	J&E	Freeze-up End	0.4	0.57	< 0.01**
Baffin Bay	J&E	Freeze-up Start	0.5	0.71	< 0.01**
Barents Sea	Bliss	Day of Advance	1.3	0.7	< 0.01**
Barents Sea	Bliss	Day of Closing	1.3	0.7	< 0.01**
Barents Sea	Bliss	Day of Opening	-1.1	-0.72	< 0.01**
Barents Sea	Bliss	Day of Retreat	-1.2	-0.79	< 0.01**
Barents Sea	J&E	Break-up End	-1.0	-0.72	< 0.01**
Barents Sea	J&E	Break-up Start	-0.4	-0.38	0.02*
Barents Sea	J&E	Freeze-up End	1.0	0.72	< 0.01**
Barents Sea	J&E	Freeze-up Start	1.0	0.8	< 0.01**
Beaufort Sea	Bliss	Day of Advance	0.8	0.61	< 0.01**
Beaufort Sea	Bliss	Day of Closing	0.9	0.63	< 0.01**
Beaufort Sea	Bliss	Day of Opening	-0.7	-0.51	< 0.01**
Beaufort Sea	Bliss	Day of Retreat	-1.0	-0.56	< 0.01**
Beaufort Sea	J&E	Break-up End	-0.7	-0.48	< 0.01**
Beaufort Sea	J&E	Break-up Start	-0.6	-0.51	< 0.01**

Beaufort Sea	J&E	Freeze-up End	0.7	0.68	< 0.01**
Beaufort Sea	J&E	Freeze-up Start	0.7	0.65	< 0.01**
Bering Sea	Bliss	Day of Advance	0.4	0.43	< 0.01**
Bering Sea	Bliss	Day of Closing	0.4	0.36	0.02*
Bering Sea	Bliss	Day of Opening	-0.2	-0.28	0.09
Bering Sea	Bliss	Day of Retreat	-0.3	-0.37	0.02*
Bering Sea	J&E	Break-up End	-0.0	-0.01	0.98
Bering Sea	J&E	Break-up Start	0.0	0.05	0.77
Bering Sea	J&E	Freeze-up End	0.3	0.33	0.04*
Bering Sea	J&E	Freeze-up Start	0.5	0.65	< 0.01**
Canadian Arch.	Bliss	Day of Advance	0.5	0.63	< 0.01**
Canadian Arch.	Bliss	Day of Closing	0.6	0.56	< 0.01**
Canadian Arch.	Bliss	Day of Opening	-0.3	-0.57	< 0.01**
Canadian Arch.	Bliss	Day of Retreat	-0.9	-0.7	< 0.01**
Canadian Arch.	J&E	Break-up End	-0.4	-0.62	< 0.01**
Canadian Arch.	J&E	Break-up Start	-0.4	-0.5	< 0.01**
Canadian Arch.	J&E	Freeze-up End	0.3	0.58	< 0.01**
Canadian Arch.	J&E	Freeze-up Start	0.2	0.51	< 0.01**
Central Arctic	Bliss	Day of Closing	0.7	0.33	0.04*
Central Arctic	Bliss	Day of Opening	-0.5	-0.17	0.31
Central Arctic	J&E	Break-up End	-1.0	-0.36	0.03*
Central Arctic	J&E	Break-up Start	-0.9	-0.31	0.06
Central Arctic	J&E	Freeze-up End	0.1	0.03	0.88
Central Arctic	J&E	Freeze-up Start	0.6	0.18	0.31
Chukchi Sea	Bliss	Day of Advance	1.0	0.75	< 0.01**
Chukchi Sea	Bliss	Day of Closing	1.1	0.73	< 0.01**

Chukchi Sea	Bliss	Day of Opening	-0.7	-0.71	< 0.01**
Chukchi Sea	Bliss	Day of Retreat	-0.7	-0.66	< 0.01**
Chukchi Sea	J&E	Break-up End	-0.6	-0.65	< 0.01**
Chukchi Sea	J&E	Break-up Start	-0.5	-0.46	< 0.01**
Chukchi Sea	J&E	Freeze-up End	0.8	0.69	< 0.01**
Chukchi Sea	J&E	Freeze-up Start	1.0	0.79	< 0.01**
E. Siberian Sea	Bliss	Day of Advance	0.8	0.74	< 0.01**
E. Siberian Sea	Bliss	Day of Closing	1.1	0.78	< 0.01**
E. Siberian Sea	Bliss	Day of Opening	-0.7	-0.51	< 0.01**
E. Siberian Sea	Bliss	Day of Retreat	-0.8	-0.6	< 0.01**
E. Siberian Sea	J&E	Break-up End	-0.5	-0.45	< 0.01**
E. Siberian Sea	J&E	Break-up Start	-0.7	-0.46	< 0.01**
E. Siberian Sea	J&E	Freeze-up End	0.6	0.76	< 0.01**
E. Siberian Sea	J&E	Freeze-up Start	0.7	0.77	< 0.01**
Greenland Sea	Bliss	Day of Advance	0.9	0.62	< 0.01**
Greenland Sea	Bliss	Day of Closing	0.5	0.45	< 0.01**
Greenland Sea	Bliss	Day of Opening	-0.4	-0.38	0.02*
Greenland Sea	Bliss	Day of Retreat	-0.6	-0.5	< 0.01**
Greenland Sea	J&E	Break-up End	-0.3	-0.32	0.05*
Greenland Sea	J&E	Break-up Start	-0.0	-0.04	0.79
Greenland Sea	J&E	Freeze-up End	0.4	0.38	0.02*
Greenland Sea	J&E	Freeze-up Start	0.7	0.63	< 0.01**

Hudson Bay	Bliss	Day of Advance	0.5	0.64	< 0.01**
Hudson Bay	Bliss	Day of Closing	0.4	0.57	< 0.01**
Hudson Bay	Bliss	Day of Opening	-0.5	-0.67	< 0.01**
Hudson Bay	Bliss	Day of Retreat	-0.7	-0.74	< 0.01**
Hudson Bay	J&E	Break-up End	-0.4	-0.65	< 0.01**
Hudson Bay	J&E	Break-up Start	-0.1	-0.06	0.72
Hudson Bay	J&E	Freeze-up End	0.4	0.55	< 0.01**
Hudson Bay	J&E	Freeze-up Start	0.6	0.73	< 0.01**
Kara Sea	Bliss	Day of Advance	0.7	0.63	< 0.01**
Kara Sea	Bliss	Day of Closing	0.9	0.66	< 0.01**
Kara Sea	Bliss	Day of Opening	-1.0	-0.75	< 0.01**
Kara Sea	Bliss	Day of Retreat	-1.1	-0.76	< 0.01**
Kara Sea	J&E	Break-up End	-0.9	-0.7	< 0.01**
Kara Sea	J&E	Break-up Start	-0.3	-0.22	0.18
Kara Sea	J&E	Freeze-up End	0.8	0.62	< 0.01**
Kara Sea	J&E	Freeze-up Start	0.7	0.64	< 0.01**
Laptev Sea	Bliss	Day of Advance	0.6	0.65	< 0.01**
Laptev Sea	Bliss	Day of Closing	0.7	0.64	< 0.01**
Laptev Sea	Bliss	Day of Opening	-0.6	-0.55	< 0.01**
Laptev Sea	Bliss	Day of Retreat	-0.7	-0.58	< 0.01**
Laptev Sea	J&E	Break-up End	-0.6	-0.52	< 0.01**
Laptev Sea	J&E	Break-up Start	-0.7	-0.48	< 0.01**
Laptev Sea	J&E	Freeze-up End	0.4	0.68	< 0.01**
Laptev Sea	J&E	Freeze-up Start	0.4	0.64	< 0.01**

1375

1376

1377 Table S3. Same as Table S2, but for the local indicators. Slopes (linear regression lines)
 1378 correspond to Figures 8-11. Also shown are the explained variances (r^2 values of the trend
 1379 lines and their levels of statistical significance.

1380

Location	Indicator Group	Indicator	Slope (days yr ⁻¹)	r ²	Significance level
Churchill	Bliss	Day of Advance	0.3	0.52	< 0.01**
Churchill	Bliss	Day of Closing	0.4	0.51	< 0.01**
Churchill	Bliss	Day of Opening	-0.8	-0.59	< 0.01**
Churchill	Bliss	Day of Retreat	-1.0	-0.67	< 0.01**
Churchill	J&E	Break-up End	-0.7	-0.54	< 0.01**
Churchill	J&E	Break-up Start	-0.5	-0.3	0.07
Churchill	J&E	Freeze-up End	0.4	0.49	< 0.01**
Churchill	J&E	Freeze-up Start	0.7	0.53	< 0.01**
Clyde River	Bliss	Day of Advance	0.3	0.46	< 0.01**
Clyde River	Bliss	Day of Closing	0.3	0.45	< 0.01**
Clyde River	Bliss	Day of Opening	-0.6	-0.47	< 0.01**
Clyde River	Bliss	Day of Retreat	-0.5	-0.42	< 0.01**
Clyde River	J&E	Break-up End	-0.6	-0.5	< 0.01**
Clyde River	J&E	Break-up Start	-0.5	-0.22	0.18
Clyde River	J&E	Freeze-up End	0.3	0.45	< 0.01**
Clyde River	J&E	Freeze-up Start	0.3	0.43	< 0.01**
Mestersvig	Bliss	Day of Advance	0.6	0.36	0.05*
Mestersvig	Bliss	Day of Closing	0.9	0.52	< 0.01**
Mestersvig	Bliss	Day of Opening	-0.7	-0.36	0.02*
Mestersvig	Bliss	Day of Retreat	-0.6	-0.37	0.04*
Mestersvig	J&E	Break-up End	-0.2	-0.2	0.26
Mestersvig	J&E	Break-up Start	0.1	0.04	0.83

Mestersvig	J&E	Freeze-up End	0.6	0.5	< 0.01**
Mestersvig	J&E	Freeze-up Start	0.5	0.42	0.02*
Pevek	Bliss	Day of Advance	1.1	0.72	< 0.01**
Pevek	Bliss	Day of Closing	1.1	0.77	< 0.01**
Pevek	Bliss	Day of Opening	-0.9	-0.4	0.01*
Pevek	Bliss	Day of Retreat	-1.0	-0.46	< 0.01**
Pevek	J&E	Break-up End	-0.7	-0.33	0.05
Pevek	J&E	Break-up Start	-1.1	-0.37	0.03*
Pevek	J&E	Freeze-up End	0.8	0.76	< 0.01**
Pevek	J&E	Freeze-up Start	0.9	0.73	< 0.01**
Prudhoe Bay	Bliss	Day of Advance	0.8	0.52	< 0.01**
Prudhoe Bay	Bliss	Day of Closing	0.8	0.65	< 0.01**
Prudhoe Bay	Bliss	Day of Opening	-1.0	-0.56	< 0.01**
Prudhoe Bay	Bliss	Day of Retreat	-0.9	-0.51	< 0.01**
Prudhoe Bay	J&E	Break-up End	-0.8	-0.54	< 0.01**
Prudhoe Bay	J&E	Break-up Start	-0.5	-0.27	0.1
Prudhoe Bay	J&E	Freeze-up End	0.8	0.6	< 0.01**
Prudhoe Bay	J&E	Freeze-up Start	0.7	0.59	< 0.01**
Sabetta	Bliss	Day of Advance	0.4	0.55	< 0.01**
Sabetta	Bliss	Day of Closing	0.4	0.47	< 0.01**
Sabetta	Bliss	Day of Opening	-0.9	-0.59	< 0.01**
Sabetta	Bliss	Day of Retreat	-1.0	-0.78	< 0.01**
Sabetta	J&E	Break-up End	-0.8	-0.56	< 0.01**
Sabetta	J&E	Break-up Start	-0.9	-0.42	< 0.01**
Sabetta	J&E	Freeze-up End	0.4	0.41	< 0.01**
Sabetta	J&E	Freeze-up Start	0.4	0.56	< 0.01**

South Chukchi Sea	Bliss	Day of Advance	0.9	0.63	< 0.01**
South Chukchi Sea	Bliss	Day of Closing	0.7	0.58	< 0.01**
South Chukchi Sea	Bliss	Day of Opening	-0.6	-0.51	< 0.01**
South Chukchi Sea	Bliss	Day of Retreat	-0.7	-0.56	< 0.01**
South Chukchi Sea	J&E	Break-up End	-0.6	-0.52	< 0.01**
South Chukchi Sea	J&E	Break-up Start	-0.6	-0.39	0.02*
South Chukchi Sea	J&E	Freeze-up End	0.7	0.57	< 0.01**
South Chukchi Sea	J&E	Freeze-up Start	0.8	0.63	< 0.01**
St. Lawrence Island	Bliss	Day of Advance	0.6	0.33	0.05*
St. Lawrence Island	Bliss	Day of Closing	0.3	0.2	0.24
St. Lawrence Island	Bliss	Day of Opening	-0.1	-0.16	0.35
St. Lawrence Island	Bliss	Day of Retreat	-0.3	-0.28	0.09
St. Lawrence Island	J&E	Break-up End	-0.1	-0.11	0.49
St. Lawrence Island	J&E	Break-up Start	-0.0	-0.02	0.92
St. Lawrence Island	J&E	Freeze-up End	0.4	0.25	0.13
St. Lawrence Island	J&E	Freeze-up Start	0.5	0.33	0.04*
Tiksi	Bliss	Day of Advance	0.2	0.36	0.02*
Tiksi	Bliss	Day of Closing	0.2	0.41	0.01*

Tiksi	Bliss	Day of Opening	-0.4	-0.54	< 0.01**
Tiksi	Bliss	Day of Retreat	-0.6	-0.54	< 0.01**
Tiksi	J&E	Break-up End	-0.3	-0.53	< 0.01**
Tiksi	J&E	Break-up Start	-0.3	-0.34	0.03*
Tiksi	J&E	Freeze-up End	0.3	0.45	< 0.01**
Tiksi	J&E	Freeze-up Start	0.2	0.45	< 0.01**
Utqiaf°vik	Bliss	Day of Advance	1.1	0.6	< 0.01**
Utqiaf°vik	Bliss	Day of Closing	1.1	0.67	< 0.01**
Utqiaf°vik	Bliss	Day of Opening	-1.2	-0.52	< 0.01**
Utqiaf°vik	Bliss	Day of Retreat	-1.2	-0.71	< 0.01**
Utqiaf°vik	J&E	Break-up End	-0.7	-0.52	< 0.01**
Utqiaf°vik	J&E	Break-up Start	-0.7	-0.27	0.11
Utqiaf°vik	J&E	Freeze-up End	0.8	0.66	< 0.01**
Utqiaf°vik	J&E	Freeze-up Start	0.9	0.62	< 0.01**

1381

1382

1383

1384

1385